Differential Functional Regulation of PKC Orthologs in Fission Yeast

Marisa Madrid[1], Beatriz Vázquez-Marín[1], Teresa Soto[1], Alejandro Franco[1], Elisa Gómez-Gil, Jero Vicente-Soler[1], Mariano Gacto[1], Pilar Pérez[2], and José Cansado[1].

[1] Yeast Physiology Group, Department of Genetics and Microbiology, Facultad de Biología, Universidad de Murcia, 30071 Murcia, Spain.
[2] Instituto de Biología Funcional y Genómica (IBFG), Consejo Superior de Investigaciones Científicas, Universidad de Salamanca, 37007 Salamanca, Spain.

Running title: *Distinct regulation of PKC isoforms*

To whom correspondence should be addressed:
Prof. José Cansado, Department of Genetics and Microbiology. Universidad de Murcia. Campus Universitario de Espinardo. 30071 Murcia, Spain; E-mail: jcansado@um.es
Dr. Marisa Madrid, Department of Genetics and Microbiology. Universidad de Murcia. Campus Universitario de Espinardo. 30071 Murcia, Spain; E-mail: marisa@um.es

Keywords: *Schizosaccharomyces pombe*, stress response, signal transduction, Rho GTPase, protein kinase C, mitogen-activated protein kinase

---

ABSTRACT

The two PKC orthologs Pck1 and Pck2 in the fission yeast *Schizosaccharomyces pombe* operate in a redundant fashion to control essential functions, including morphogenesis and cell wall biosynthesis, as well as the activity of the cell integrity pathway (CIP) and its core element the MAPK Pmk1. We show here that despite the strong structural similarity and functional redundancy of these two enzymes, the mechanisms regulating their maturation, activation, and stabilization have a remarkably distinct biological impact on both kinases. We found that in contrast to Pck2, putative in vivo phosphorylation of Pck1 within the conserved activation loop, turn and hydrophobic motifs is essential for Pck1 stability and biological functions. Constitutive Pck activation promoted dephosphorylation and destabilization of Pck2, while it enhanced Pck1 levels to interfere with proper downstream signaling to the CIP via Pck2. Importantly, whereas catalytic activity was essential for Pck1 function, Pck2 remained partially functional independently of its catalytic activity. Our findings suggest that early divergence from a common ancestor in fission yeast involved important changes in the mechanisms regulating catalytic activation and stability of PKC family members to allow for flexible and dynamic control of downstream functions, including MAPK signaling.

The Protein Kinase C family of isozymes plays essential roles in signalling pathways controlling cell growth, proliferation, differentiation, and cell death (1,2). Classical, novel and atypical mammalian PKC isoforms share a basic structure with a variable N-terminal regulatory domain followed by a highly conserved C-terminal kinase domain, which

contains three conserved phosphorylation sites critical for catalytic activity: activation loop (AL), turn motif (TM), and hydrophobic motif (HM) (1,2). AL phosphorylation is essential for the catalytic activation of most PKCs isoforms, and is carried out by 3-phosphoinositide-dependent kinase-1 (PDK-1) (1,2). The mammalian target of rapamycin (mTOR) or an autophosphorylation mechanism mediate TM and HM phosphorylation of most PKCs, although their requirement to regulate kinase activity varies among different family members (2). Given their essential biological roles, PKC isozymes are present throughout the eukaryotic lineage from humans to simple organisms like yeasts (3). Indeed, the budding yeast *Saccharomyces cerevisiae* harbors a single and essential PKC ortholog named Pkc1, whose phosphorylation at T-983 within AL by redundant PDKs Pkh1 and Pkh2 is indispensable for its catalytic and biological functions (4).

The fission yeast *Schizosaccharomyces pombe* has two non-essential PKC orthologs known as Pck1 and Pck2 (5,6). Both kinases share extensive homology at their amino-acid sequences, particularly within the catalytic domain (~70% identity within 180 amino acids; Fig. 1). Both Pck1 and Pck2, as *S. cerevisiae* Pkc1, retain the regulatory C1 and C2 domains found in mammalian PKCs, but present an extended regulatory domain including two polybasic coiled-coil HR1 domains that mediate binding and regulation by GTP-bound Rho GTPase family members Rho1 and Rho2 (Fig. 1A) (7,8). HR1 domains in Pkc1 and Pck1/Pck2 are closely related to those present in mammalian Rho family-responsive PKN kinases PKN1-3, a subfamily within the PKC family that binds and become regulated by Rho family members (9). Pck1 and Pck2 are short half-life proteins that contain N-terminal PEST sequences, and their interaction with either GTP-Rho1 or GTP-Rho2 increases their stability (7,8). Rho1 and Rho2 synergistically regulate through Pck1 and Pck2 the biosynthesis of (1,3) β-D-glucan and α-glucan, which are the two main cell wall polymers in fission yeast (7,10). Pck1 and Pck2 share overlapping roles in cell viability, partially complement each other, and their simultaneous deletion elicits a synthetic lethal phenotype (7,10).

Besides its role controlling glucan synthesis, Pck2 is a major upstream activator of the cell integrity MAP kinase pathway (CIP). Its core component, MAP kinase Pmk1, becomes activated during growth and in response to adverse environmental conditions and regulates several processes, including cell separation, cell wall construction, or ionic homeostasis (5,6,11). Whereas the Rho2-Pck2 branch is essential for Pmk1 activation in response to hyper- and hypo-osmotic stress, both Rho1 and Rho2 target Pck2 to activate the CIP during vegetative growth and cell wall damage (12) (Fig. 1B). The PDK ortholog Ksg1 and an autophosphorylation mechanism are responsible for the in vivo phosphorylation of Pck2 at the conserved T842 within the activation loop (AL) during vegetative growth and under stress (13). These events together with turn motif autophosphorylation at T984 and binding to Rho1 and/or Rho2 stabilizes and render Pck2 competent to exert its biological functions including activation of the CIP (13). In addition, we have discovered a novel mechanism involving Akt ortholog Gad8 (TORC2 complex target) and Psk1 (TORC1 target) which promotes an increase in Pck2 protein levels to allow activation of the CIP in response to cell wall damage or glucose exhaustion (14,15).

Initial observations suggested that Pck1 was a negative regulator of the CIP (16). However, later studies demonstrated that, instead, it plays a less prominent role than Pck2 as a positive regulator of Pmk1 activity during

vegetative growth and cell wall stress (12,16). Nevertheless, considering their shared functions and strong structural similarity, it might be foreseen that the mechanisms regulating Pck1 function should be identical to those described for Pck2. Contrary to this prediction, in this work we show that in fission yeast the expansion of the PKC family from a single ancestor was accompanied by striking differences in the mechanisms regulating maturation, activation, and protein levels of both kinases. The early acquisition of differential regulatory activation and stabilization by Pck1 and Pck2 allows for fine tuning of downstream MAPK signaling and regulation of cellular homeostasis in this simple organism.

RESULTS

Pck1 is phosphorylated in vivo *by Ksg1 within AL at T823 and is more stable than Pck2*- The C-terminal catalytic domains of Pck1 and Pck2 are strongly conserved (Fig. 1A). We showed previously that the conserved threonine-842 located at Pck2 activation loop (AL) is phosphorylated in vivo by the PDK1 ortholog Ksg1 (14). The equivalent threonine residue within Pck1 AL lies at position 823 (Fig 1). Using a specific anti-phospho-T823 antibody (see Materials and Methods), we detected specific in vivo phosphorylation of Pck1 at this residue (Suppl. Fig 1). Incubation with anti-phospho-T823 antibody revealed a strong phosphorylation signal by in vitro kinase assays performed with wild type versions of Ksg1 and Pck1 (Fig. 2A, lane 4). This signal was totally absent when employing the kinase-dead version of Ksg1 (Fig. 2A, lane 5), or a T823A mutated version of Pck1 (Fig. 2A, lane 6), thus showing that Ksg1 phosphorylates Pck1 AL at T823 in vitro. To explore the functional relationship between Ksg1 and Pck1 phosphorylation at T823 in vivo we obtained control and *ksg1-208* strains expressing genomic Pck1-HA tagged versions in a *pck1Δ* background. The *ksg1-208* allele shows normal growth at 25ºC and thermosensitive phenotype above 34.5ºC. *ksg1-208* cells show marked morphology defects and sensitivity to staurosporine, a potent PKC inhibitor (17). In control cells the levels of total (anti-HA antibody) and T823-phosphorylated Pck1 were ~10x higher than in *ksg1-208* cells either growing at the permissive temperature (25ºC), or incubated at 36ºC, which is a restrictive temperature for Ksg1 function (Fig. 2B). These results indicate that Ksg1 is also responsible for AL phosphorylation of Pck1 at T823 in vivo, and this event might regulate Pck1 stability (see below).

Pck2 protein levels increase in response to different stresses through a mechanism partially regulated by the TORC2 complex and its main component Tor1 kinase (14,15). We found that both total and T823-phosphorylated Pck1 levels were ~2 or 3-fold lower in growing *tor1Δ* cells as compared to control cells (Fig. 2C). Both T823-phosphorylated and total Pck1 levels augmented progressively in control cells subjected to a saline stress (KCl), a cell wall stress with Caspofungin (a specific β-glucan synthase inhibitor), or after starvation from glucose (Fig. 2C). Importantly, such rise was strongly abrogated in *tor1Δ* cells during cell wall stress or glucose starvation, while being less evident in response to a salt stress (Fig. 2C). Taken together, these findings suggest that the TORC2 complex upregulates Pck1 levels during growth and in response to specific stresses.

Total Pck1 protein levels were approximately 2 or 3-fold higher than those of Pck2 (Fig. 2D, time 0), confirming previous data on absolute proteome quantifications at single cell level (18). Remarkably, in contrast to Pck2, which is a relatively unstable protein with short half-life (14), Pck1 protein levels decreased very

slowly in growing cells treated with the protein synthesis inhibitor cycloheximide (Fig. 2E), implying that Pck1 is more stable than the Pck2 isoform.

Putative phosphorylation at conserved AL, TM and HM residues differentially affects Pck1 and Pck2 levels and biological functions-In fission yeast total Pck2 levels are very similar in control cells and in those expressing a non-phosphorylatable AL mutant (Pck2-*T842A*; Fig. 3A) (14). However, the observation that both total and T823-phosphorylated Pck1 levels are quite low in *ksg1-208* cells suggested that Pck1 stability is dependent upon AL phosphorylation. Indeed, as shown in Fig. 3B, Pck1 levels were strongly reduced by approximately 95% in cells expressing the unphosphorylated AL mutant Pck1-*T823A*. Similar to Pck2 (14), bacterially purified or immunoprecipitated versions of wild type and Pck1 mutants were not active either in vitro or in vivo, thus preventing for a direct biochemical confirmation of their kinase activity status. Instead, we tested the ability of genomic versions of wild type or mutated alleles of Pck1 to suppress several known phenotypes of *pck1Δ* cells, including defective signaling to the CIP and growth sensitivity in the presence of Caspofungin, Calcofluor white, and magnesium chloride (12,16), as biological readouts to comparatively asses their function in vivo. The *T842A* mutation does not affect Pck2 signalling activity to the CIP or growth sensitivity in the presence of Caspofungin (Fig. 3C) (14). On the contrary, as compared to control cells, *pck1-T823A* cells displayed a strong or moderate growth sensitive phenotype in presence of Caspofungin, magnesium chloride, and Calcofluor white (Fig. 3C). Pck1-T823A was also synthetic lethal with the *pck2Δ* mutation (not shown). Thus, in vivo AL phosphorylation is a critical determinant for stability and biological functions of Pck1, but not in the case of the Pck2 ortholog. We also noticed that the growth sensitivity of *pck1-T823A* cells to the above stressors was more pronounced than in *pck1Δ* cells (Fig. 3C). While overexpression of wild type Pck2 alters cell morphology and inhibits fission yeast growth due to hyperactivation of the CIP, overexpression of the *pck2-T842A* allele is not lethal (Fig. 3D) (19). Contrariwise, overexpression of wild type Pck1 is not lethal (12), whereas overexpression of the Pck1-*T823A* mutant allele induced a strong lytic phenotype and was deleterious for cell growth (Fig. 3D). Moreover, the maximal activation of the CIP core member MAPK Pmk1 in response to a salt stress, which is exclusively dependent upon Pck2 function (16), showed a modest but significant decrease in *pck1-T823A* cells as compared to control cells (Fig. 3E). Collectively, these results suggest that Pck1 requires to be phosphorylated in vivo within the AL by Ksg1 to attain a stable and functional conformation, and that failure to do so may negatively interfere with proper Pck2 signaling.

Together with the canonical AL site at T842, T846 has been proposed to be phosphorylated in vivo and to play a role on the Pck2 catalytic activation and biological functions (14). Both total and T823-phoshorylated Pck1 levels were unaffected in cells expressing Pck1-*T827A* with a mutation in the amino acid residue equivalent to Pck2-*T846A* (Fig. 1A; Fig. 3B). However, this Pck1 mutant was as sensitive as *pck1Δ* cells to Calcofluor white and magnesium chloride, but not to Caspofungin (Fig. 3C). Conversely, mutation of Pck1 within the conserved phosphorylatable TM site (Pck1-*T965A*) decreased both total and T823-phosphorylated kinase levels (Fig. 3B), and resulted in growth sensitivity only to Caspofungin (Fig. 3F). Hence, in vivo putative phosphorylation of Pck1 at T827 (AL) and T965 (TM) may positively influence Pck1 biological

functions under specific biological contexts. Mutation at the putative conserved phosphorylation site within Pck1 HM (Pck1-*S983A*), did not affect Pck1 stability, AL phosphorylation, or biological functions (Fig. 3B and 3F). However, in sharp contrast with Pck2, the Pck1 mutant at both TM and HM (Pck1-*T965A S983A*), which is equivalent to Pck2-*T984A S1002A* mutant, showed very low protein levels (~80% decrease as compared to control cells; Fig. 3B), and its sensitivity to different stresses was similar to that of *pck1Δ* cells (Fig. 3F). Taken as a whole, these observations reinforce the idea that, contrary to Pck2, in vivo phosphorylations of Pck1 within AL, TM and HM sites are essential for protein stability and biological functions.

Mutation at conserved pseudosubstrate motif has distinct effects on Pck1 and Pck2 stability and downstream signaling-PKCs, including PKCα, possess a pseudosubstrate segment (PS) that keeps the enzyme in a closed autoinhibited conformation. This domain blocks the substrate binding cavity and protects the priming AL, TM and HM phospho-sites within the catalytic domain from dephosphorylation (20). Deletion of the PS domain or a point mutation in the conserved alanine residue to a negatively charged glutamic acid renders constitutively active the kinase both in vivo and in vitro (21). Both Pck1 and Pck2 also harbor a PS domain with conserved alanine residues at positions 399 and 392, respectively (Fig 4A). We found that total and P-T842 Pck2 levels were ~40% lower in the PS mutant (*pck2-A392E*) than in control cells (Fig 4B). This finding was somehow expected, since it is assumed that constitutive catalytic activation of PKCs elicits its subsequent dephosphorylation and degradation (22). Remarkably, Pmk1 phosphorylation was enhanced in growing *pck2-A392E* cells as compared to control cells (Fig 4C), and this feature was accompanied by increased growth sensitivity to magnesium chloride (Fig 4D), which is a known phenotype associated to increased basal Pmk1 activity (23). The increase in total Pck2 abundance displayed by control cells when treated with a cell wall synthesis inhibitor (Caspofungin) or KCl (salt stress) was reduced by approximately 50-55% in *pck2-A392E* cells (Fig 4E). Pmk1 activation in the presence of Caspofungin was partially defective in *pck2-A392E* cells (Fig 4F), although they were not hypersensitive to this compound (Suppl. Fig. S2). In contrast, the response to a salt stress was similar to control cells expressing $pck2^{+}$ (Fig 4F). Taken together, these observations support the hypothesis that constitutive activation promotes dephosphorylation and destabilization of Pck2, resulting in increased basal Pmk1 activity and limited downstream signaling to the CIP in conditions that require *de novo* protein synthesis like cell wall stress (13).

Contrary to Pck2, the Pck1 PS mutant (*pck1-A399E*) showed total and T823-phosphorylated levels that were approximately twice that of control cells expressing $pck1^{+}$ (Fig 5A). Interestingly, both total and T823-phosphorylated Pck1 levels, which increase progressively in control cells in response to a cell wall or salt stress, did not increase further in *pck1-A399E* cells under the same treatments, but dropped slowly with longer incubation times (Fig 5B). Pck2 plays a prominent role in the activation of the CIP during vegetative growth, whereas Pck1 contribution to this response is minimal, as seen by the strong drop in basal Pmk1 phosphorylation detected in *pck2Δ* cells as compared to control cells (Fig 5C) (16). However, *pck1-A399E* cells showed a marked increase in basal Pmk1 phosphorylation that was only partially attenuated in absence of Pck2 (~50% reduction in *pck1-A399E pck2Δ* cells

versus ~80% in *pck2Δ* cells expressing wild type Pck1) (Fig 5C). Growth sensitivity to magnesium chloride mirrored the basal Pmk1 phosphorylation levels displayed by these mutant strains (Fig. 5D). Interestingly, Pck2-mediated activation of Pmk1 in response to salt stress, which is independent of Pck1 function (16), was attenuated in *pck1-A399E* cells (Fig 5E). Therefore, constitutive catalytic activation of Pck1 might interfere with proper downstream signaling of Pck2 to the MAPK Pmk1.

Exponentially growing fission yeast cultures show 20-25% of septated cells (*Control*; Fig. 5F and G). Remarkably, *Pck1-A399E* cells showed strong cytokinesis defects, with a notable increase in both septated and multiseptated cells (~50% and ~5% of total cell number, respectively; Fig. 5F and G). Constitutive activation of Pmk1 appears to be responsible for this defect, since it was mostly suppressed by simultaneous deletion of Pmk1 (Fig. 5F and G). However, despite the functional relationship between constitutive Pck1 activity and Pmk1 function, overexpression of Pck1-*A399E* was lethal in either control or *pmk1Δ* cells (Fig. 5H), suggesting that Pck1 can modulate morphogenesis and/or cell growth through both Pmk1-dependent and -independent mechanisms.

Pck1 is a main Rho1 effector during the control of cell growth and cell integrity signaling-The essential Rho GTPase Rho1 is involved together with Rho2 in the activation of the CIP during vegetative growth and in response to cell wall damage (12). Cells expressing the hypomorphic Rho1 allele *rho1-596* show a thermosensitive phenotype and are hypersensitive to Caspofungin (Fig. 6A) (24). Notably, both phenotypes were partially suppressed by the Pck1-*A399E* PS mutated protein (Fig. 6A). The high percentage in septated and multiseptated cells present in the *Pck1-A399E* mutant (~50% and ~5%, respectively), was alleviated in a *rho1-596 pck1-A399E* background (~27% and ~0.5% of septated and multiseptated cells, respectively; Fig. 6B). On the contrary, *rho1-596* thermosensitivity was aggravated by the simultaneous presence of the equivalent Pck2-*A392E* mutated protein (Suppl. Fig. S2). The low total and P-T823 Pck1 levels present in *rho1-596* cells during growth and in response to stress (KCl) were partly restored in a *rho1-596 pck1-A399E* double mutant strain (Fig 6C). The increase in basal Pmk1 phosphorylation displayed by the *rho1-59*6 hypomorphic allele (24), and *pck1-A399E* cells (Fig 5C), was significantly reduced in a *rho1-596 pck1-A399E* background (Fig 6D). Moreover, the enhanced Pmk1 activity displayed by *pck1-A399E* cells was strongly alleviated in a *rho1-596 rho2Δ* double mutant as compared to *rho2Δ* cells (Fig. 6E). Altogether, these results support the functional relevance of activated Pck1 as a main Rho1 effector during the control of cell growth and cell integrity signaling.

Catalytic activity is essential for Pck1 but not Pck2 function, and promotes destabilization of both kinases- To gain more insight on how catalytic activation of Pck1 and Pck2 affects their stability and functions, we generated strains expressing catalytic inactive Pck1-*D789N* and Pck2-*D808N*, in which the conserved catalytic aspartate was substituted by asparagine, thus maintaining the integrity of the ATP binding pocket (Fig. 7A) (25). Mammalian PKCs carrying this mutation are constitutively phosphorylated (primed) within AL, TM, and HM as they become protected from dephosphorylation (25). As compared to control cells, total and P-T842 Pck2 levels were detected in cells carrying *pck2-D808N* as shifted/slower migrating bands reminiscent of increased phosphorylation (Fig. 7B), and the total amount of either Pck2-*D808N* or Pck2-*A392E D808N* was approximately twice that of control cells.

Importantly, the difference in T842 phosphorylation was negligible in both *pck2-D808N* cells and in a *pck2-A392E D808N* double mutant (Fig. 7B), suggesting that intrinsic catalytic activity is responsible for destabilization triggered after activation of Pck2. These mutants also showed very low basal Pmk1 phosphorylation (Fig. 7C). Moreover, Pck2-*A392E D808N* cells failed to activate Pmk1 in response to salt stress, confirming that catalytic activation of Pck2 is essential for this response (Fig. 7D). Similar to the *pck2-D808N* mutant, total and P-T823 Pck1 levels were present in *pck1-D789N* cells as multiple species with reduced electrophoretic mobility, and the total amount of either Pck1-*D789N* or Pck1-*A399E D789N* was approximately two times higher than in control cells (Fig 7E). Notably, introduction of the *D789N* mutation in *pck1-A399E* suppressed both the increase in Pmk1 activity and the multiseptated phenotype shown by cells expressing the constitutively active PS mutant (Fig. 7F and G). The negative effect of the *D789N* mutation was evident as the growth sensitivity to Caspofungin of both *pck1-D789N* and *pck1-A399E D789N* cells were even higher than in *pck1Δ* cells (Fig. 7H). However, contrary to *pck2Δ* cells, *pck2-D808N* and *pck2-A392E D808N* cells were moderately growth resistant in the presence of this compound (Fig 7I). Therefore, while Pck1 functions appear strictly dependent upon its catalytic activity, inactive Pck2 is biologically functional to a certain extent. Our results also indicate that intrinsic kinase activity promotes destabilization of both Pck1 and Pck2.

DISCUSSION

The PKC orthologs Pck1 and Pck2 share an essential role to modulate cell growth and morphogenesis in fission yeast (6,7). Taking into account their redundant functions and strong structural similarity in the regulatory and catalytic domains, it might be anticipated that the mechanisms responsible for catalytic activation and stabilization of both kinases should be identical. We found that similar to Pck2 (14) and most PKC isoforms from higher eukaryots (2,26), the conserved threonine-823 within the AL of Pck1 becomes phosphorylated in vivo by Ksg1, the fission yeast PDK ortholog. We also confirmed that, as in Pck2, the TORC2 complex plays a major role to positively regulate Pck1 levels during growth and in response to most stresses. Notably, Pck1 upregulation was clearly abrogated in *tor1Δ* cells during cell wall stress or glucose starvation, but was only slightly limited during salt stress. The nature of the above stresses is very different, and therefore it is likely that this specific treatment was not of enough strength for the effect to manifest in a clear fashion. In any case, despite the above similarities, we provide compelling evidence that regulation of catalytic activation and stabilization of Pck1 and Pck2 has a remarkably distinct biological impact on both kinases (Fig. 8).

The intracellular levels of most mammalian PKCs are strongly reduced in the absence of AL phosphorylation (2). For example, PKCα AL dephosphorylation decreases its sumoylation, which in turn promotes its ubiquitination and ultimately enhances its degradation via the ubiquitin-proteasome pathway (27). We observed that Ksg1-dependent in vivo AL phosphorylation is also a major mechanism controlling Pck1 stability and biological functions. In strong contrast, Pck2 protein levels, downstream signalling to the CIP, and biological functions are not significantly altered in the non-phosphorylatable AL mutant Pck2-*T842A* with respect to control cells (14). Moreover, whereas individual and/or combined mutations at the putative in vivo phosphorylation

TM and HM sites had an overall negative effect on Pck1 levels and function, this effect was not shown in the respective Pck2 mutant counterparts. Hence, fission yeast Pck1 resembles the majority of mammalian PKC family members, where maturation is dependent upon phosphorylation at conserved AL, TM, and HM sites within the catalytic domain, and converts newly synthesized kinases into a stable degradation-resistant conformation (1). Our results also suggest that newly synthesized Pck1 is constitutively phosphorylated by PDK (Ksg1) at the AL residue (T823), and that failure to do so downregulates Pck2 signaling to the CIP. Although presently unknown, this putative interference mechanism might be due to PDK trapping by the unphosphorylatable *pck1-T823A* mutant and the ensuing defect in Pck2 activation. Contrariwise, the fact that the *pck2-T842A* mutant is stable and functional, strongly suggest that in wild type cells Pck2 might exist as both AL-phosphorylated and -unphosphorylated isoforms (Fig. 8).

Mammalian PKCs bear a pseudosubstrate segment that blocks the substrate binding cavity and protects the priming AL, TM, and HM phospho-sites within the catalytic domain from dephosphorylation and destabilization (1,20). This model predicts that deletion or a point mutation of the PS domain constitutively activates the kinase and elicits its dephosphorylation and degradation, as shown for several PKC isoforms. Introduction of the PS mutation in Pck2 (*pck2-A392E* cells) increased its function as upstream activator of the CIP during vegetative growth, but at the same time promoted the destabilization of the kinase. The mechanism/s responsible for Pck2 degradation might thus be similar to those present in mammalian PKCs. Remarkably, constitutive activation in the *pck1-A392E* PS mutant also enhanced its activity but, in contrast to Pck2, increased Pck1 phosphorylation and stability. Considering that the half-life of Pck1 is longer than that of Pck2, our observations depict a model where activated Pck2 might be prone to rapid dephosphorylation and degradation whereas Pck1 is not (Fig. 8).

Nucleotide pocket occupation, but not intrinsic kinase activity, is necessary for PKC priming and maturation, since kinase-inactive mutants that maintain the integrity of the ATP binding pocket are constitutively primed (25). Similarly, autophosphorylation does not compromise phosphorylation and maturation of Pck1 and Pck2, as confirmed after introducing in both kinases the catalytic aspartate mutation (*D789N* and *D808N* mutants, respectively). Importantly, intrinsic catalytic activity is determinant for destabilization triggered after constitutive activation of Pck2, as evidenced by the recovery in phosphorylated and total Pck2 levels by *pck2-A392E D808N* cells in comparison with the single pseudosubstrate *pck2-A392E* mutant cells. In addition, the use of fully primed catalytic aspartate mutants described above allows to formally demonstrates that, whereas catalytic activity is essential for Pck1 functions, Pck2 remains partially functional in the absence of intrinsic kinase activity. Our findings suggest that the existence of biological functions without kinase activity represents a common theme within the extended PKC superfamily and might be attained early during evolution.

All the structural and regulatory elements that appear distributed among the members of the large mammalian PKC family are present in Pkc1, the single and archetypal PKC enzyme present in *S. cerevisiae* (3). For the most part, this domain structure is similarly conserved in fission yeast Pck1 and Pck2 (Fig. 1A). Therefore, from an evolutionary perspective, these two functionally redundant

kinases may represent a prime example in the expansion of the PKC superfamily from a common and single ancestor. Most importantly, our results strongly suggest that in fission yeast PKC duplication was accompanied by changes in the mechanisms that regulate catalytic activation and stability of the two kinase isoforms. The biological relevance of these distinct regulatory mechanisms is exemplified when MAPK Pmk1 activity is used as readout for Pck1 and Pck2-dependent downstream signaling. Strong Pmk1 activation in response to osmotic saline stress is a quick and transient event, does not require new protein synthesis, and is totally dependent on Pck2 catalytic activity (13,14). Indeed, Pck2 appears perfectly suited to perform this role since, contrary to Pck1, constitutive activation elicits its dephosphorylation and degradation, thus decreasing the magnitude of the signal at long incubation times. However, Pmk1 activation under cell wall stress takes place in a progressive manner until reaching its maximum at long incubation times, and depends upon the enhanced synthesis and activity of both Pck1 and Pck2 (12,14). In this situation, catalytic activation and induced stabilization of Pck1 might lead to a graded and robust downstream signaling to the MAPK module which increases with time. Differential regulation of Pck1 and Pck2 activation and/or stability may be important for the distinct roles of both kinases during cellular response to short versus longer term stress. We found that, as compared to control cells, *pck2Δ* cells exhibited a defective growth recovery phenotype after being subjected to a severe thermal stress (55ºC) during relatively short periods of time (Fig. S3). Notably, as compared to control cells, we found that *pck2Δ* cells exhibited a defective growth recovery phenotype in response to heat-shock, whereas cells expressing AL (*T842A*) and catalytically inactive (*D808N*) Pck2 alleles showed a fairly good growth recovery under the same conditions (Fig. S3). On the other hand, the equivalent Pck1 mutants showed a similar and very modest growth defect as compared to control cells (Fig. S3). These results reinforce the suggestion that both catalytically active and inactive Pck2 isoforms might have a more prominent role than Pck1 in promoting cell survival in response to short-term stresses. At the same time, Pck1 and Pck2 activation status must be tightly coordinated in vivo, as indicated by the observation that cells expressing the upregulated *pck1-A392E* allele hyperactivate the CIP constitutively in a Pck2-independent fashion, and interfere with proper downstream signaling to the MAPK cascade by Pck2.

In higher eukaryotes precise control of the amplitude of PKC signaling is essential for cellular homeostasis, and the disruption of this control may lead to different pathophysiological states (28). Our results suggest that alternative regulation of both kinases stability and PDK-mediated phosphorylation emerged as major factors to allow for a precise control of PKC signaling during the early diversification of this large and functionally relevant class of enzymes.

EXPERIMENTAL PROCEDURES

Strains, media, growth conditions and gene disruption-S. pombe strains used in this work (Table S1) derive from control strain MI200 which express a genomic Pmk1-HA fusion (11). They were grown in rich (YES) or minimal (EMM2) medium with 2% glucose plus supplements (29). Transformants expressing pREP3X-based plasmids were grown in liquid EMM2 medium with thiamine (5 mg/L), and either plated in solid medium with or without the vitamin, or transferred to EMM2 lacking thiamine.

Gene fusion, site-directed mutagenesis, and expression plasmids-To construct integrative plasmid pJK148-Pck1:HA, the *pck1*$^+$ ORF plus regulatory sequences was amplified by PCR using fission yeast genomic DNA as template and 5´-oligonucleotide Pck1.XbaI-F (Table S2), which hybridizes 882 to 862 bp upstream of the *pck1*$^+$ ATG start codon and contains a *Xba*I site, and 3´-oligonucleotide Pck1HASmaI-R, which hybridizes at the 3' end of *pck1*$^+$ ORF and incorporates a 64 nucleotide sequence encoding one HA epitope (sequence GYPYDVPDYA) and a *Sma*I site. PCR fragments were digested with *Xba*I and *Sma*I and cloned into integrative plasmid pJK148. Pck1 ORF contains a *Nru*I site which was deleted using the mutagenic 5'-oligonucleotide Pck1NruIX-F and the 3'-oligonucleotide Pck1NruIX-R with plasmid pJK148-Pck1:HA as template. The mutagenized Pck1 sequence was digested with *Xba*I and *Sma*I and subcloned to generate pJK148-Pck1NruIΔ:HA. Integrative plasmids expressing HA-fused Pck1 mutants were obtained by site directed mutagenesis PCR using plasmid pJK148-Pck1NruIΔ:HA as template and the mutagenic oligonucleotide pairs described in Table S2. Once confirmed, the mutagenized Pck1 sequences were subcloned into pJK148. The resulting integrative plasmids were digested at the unique *Nru*I site within *leu1*$^+$, and transformed into *pck1Δ* strain GB35 (Table S1). Transformants *leu1*$^+$ were obtained and the fusions verified by both PCR and Western blot analysis. Integrative plasmids pJK148-Pck2.A392E:HA and pJK148-Pck2.D808N:HA were obtained by site directed mutagenesis PCR using plasmid pJK148-Pck2NruIΔ:HA (14) as template, and the mutagenic oligonucleotide pairs described in Table S2. Mutant Pck1 overexpression constructs were obtained by site directed mutagenesis PCR using plasmid pREP3X-*pck1*$^+$ (7) as template and the correspondent mutagenic oligonucleotide pairs (Table S2).

A GST-fused wild type Pck1 construct was obtained by PCR employing a fission yeast cDNA library as template and the oligonucleotides Pck1pKG-F (*Sma*I site) and Pck1pKG-R (*Xba*I site). The PCR product was then digested with *Sma*I and *Xba*I and cloned into plasmid pGEX-KG (30) to generate pGEX-KG-Pck1. Mutant Pck1 constructs were obtained by site directed mutagenesis using pGEX-KG-Pck1 as template and the corresponding mutagenic oligonucleotide pairs (Table S2), digested with *Sma*I and *Xba*I, and cloned into pGEX-KG. Ksg1-GST fusion was obtained by PCR employing the oligonucleotide pair Ksg1pKG-F (*Sma*I site) and Ksg1pKG-F (*Nco*I site). A kinase dead version of Ksg1 (*K128R* mutant) was obtained by site directed mutagenesis with plasmid pGEX-KG-Ksg1 as template (14) and the mutagenic oligonucleotides Ksg1K128R-F and Ksg1K128R-R (Table S2). Constructs were digested with *Sma*I and *Nco*I and cloned into pGEX-KG.

Kinase assays-In vitro kinase reactions were performed as previously described (31), with purified bacterially expressed GST-Ksg1 or GST-Ksg1-*K128R* (kinase dead) as activating kinases, and either wild type or mutant GST-fused Pck1 constructs as substrates. GST tagged fusions were detected with polyclonal goat anti-GST antibody conjugated to horseradish peroxidase (GE Healthcare) and the ECL system.

Stress treatments and detection of activated Pmk1-Log-phase cell cultures (OD_{600}= 0.5) were supplemented with either KCl (Sigma Chemical), Caspofungin (Sigma Chemical), or Calcofluor white (Sigma Chemical). In glucose starvation experiments cells grown in YES medium with 7% glucose were resuspended in the same medium lacking glucose and osmotically equilibrated with 3% glycerol.

Preparation of cell extracts, purification of HA-tagged Pmk1 with Ni^{2+}-NTA-agarose beads (Qiagen), and SDS-PAGE was performed as described (11). Dual phosphorylation in Pmk1 was detected with rabbit polyclonal anti-phospho-p44/42 (Cell Signaling), whereas total Pmk1 was detected with mouse monoclonal anti-HA antibody (12CA5, Roche Molecular Biochemicals). Immunoreactive bands were revealed with anti-rabbit or anti-mouse-HRP-conjugated secondary antibodies (Sigma) and the ECL system (Amersham-Pharmacia).

Detection of total and phosphorylated Pck1 and Pck2-Cell extracts were prepared using Buffer IP (50 mM Tris-HCl (pH 7.5), 5 mM EDTA, 150 mM NaCl, 1 mM β-mercaptoethanol, 10% glycerol, 0.1 mM sodium orthovanadate, 1% Triton X-100, and protease inhibitors). Equal amounts of total protein were resolved in 6% SDS-PAGE gels and transferred to Hybond-ECL membranes. AL phosphorylation of Pck2 at T842 was detected using a specific anti-phospho T842 antibody as previously described (14). To detect AL phosphorylation of Pck1 at T823, an anti-phospho-polyclonal antibody was produced by immunization of rabbits with a synthetic phospho-peptide corresponding to residues surrounding T823 of Pck2 (GenScript). Total Pck2 and Pck1 were detected with mouse monoclonal anti-HA antibody. Anti-PSTAIR (anti-Cdc2, Sigma Chemical) was used for loading control.

Quantification of Western blot experiments and reproducibility of results-Densitometric quantification of Western blot signals as of 16-bit .jpg digital images of blots was performed using ImageJ (32). Briefly, bands plus background were selected or drawn as rectangles and a profile plot was obtained for each band (peaks). To minimize the background noise in the bands, each peak floating above the baseline of the corresponding profile plot was manually closed off using the straight-line tool. Finally, measurement of the closed peaks was performed with the wand tool. Relative Units for Pmk1 activation were estimated by determining the signal ratio of the anti-phospho-P44/42 blot (activated Pmk1) with respect to the anti-HA blot (total Pmk1) at each time point. Relative Units for phosphorylated and total Pck1/Pck2 levels were estimated by determining the signal ratio of either anti-phospho-P842 (AL-phosphorylated Pck2), anti-phospho-P823 (AL-phosphorylated Pck2), or anti-HA blot (total Pck2 or Pck1) with respect to the anti-cdc2 blot (internal control) at each time point. Unless otherwise stated, results shown correspond to experiments performed as biological triplicates. Mean relative units $\pm$ SD and/or representative results are shown. *P*-values were analyzed by unpaired Student´s *t* test.

Plate assay of stress sensitivity for growth-Decimal dilutions of *S. pombe* control and mutant strains were spotted per duplicate on YES solid medium or in the same medium supplemented with different concentrations of $MgCl_2$ (Sigma Chemical), FK506 (Alexis Biochemicals), Calcofluor white, or Caspofungin. Plates were incubated at 28ºC for 3 days and then photographed. Results representative of three independent experiments are shown in the corresponding Figures.

Fluorescence microscopy-Calcofluor white was employed for cell wall/septum staining as described (18). Images were taken on a Leica DM 4000B fluorescence microscope with a 100x objective and captured with a cooled Leica DC 300F camera and IM50 software. To determine the percentage of multiseptated cells, the number of septated cells was scored in each case ($n \geq 400$).

Acknowledgements: We thank F. Garro for technical assistance.

Competing interests: The authors declare that they have no conflicts of interest with the contents of this article.

Author contributions: MM and JC conceived and designed the experiments. MM, BV-M, TS, AF, JV-S, and EG-G performed the experiments. MM, PP, MG and JC analyzed the results and prepared the Figures. JC wrote the main manuscript text with input from MM, PP, and MG. All authors reviewed and approved the final version of the manuscript.

REFERENCES

1. Newton, A. C. (2010) Protein kinase C: poised to signal. *Am. J. Physiol. Endocrinol. Metab.* **298**, E395-E402
2. Freeley, M., Kelleher, D., and Long, A. (2011) Regulation of Protein Kinase C function by phosphorylation on conserved and non-conserved sites. *Cell. Signal.* **23**, 753-762
3. Mellor, H., and Parker, P. J. (1998) The extended protein kinase C superfamily. *Biochem. J.* **332**, 281-292
4. Roelants, F., Torrance, P., and Thorner, J. (2004) Differential roles of PDK1- and PDK2-phosphorylation sites in the yeast AGC kinases Ypk1, Pkc1 and Sch9. *Microbiology* **150**, 3289-3304
5. Toda, T., Dhut, S., SupertiFurga, G., Gotoh, Y., Nishida, E., Sugiura, R., and Kuno, T. (1996) The fission yeast pmk1(+) gene encodes a novel mitogen-activated protein kinase homolog which regulates cell integrity and functions coordinately with the protein kinase C pathway. *Mol. Cell. Biol.* **16**, 6752-6764
6. Perez, P., and Cansado, J. (2010) Cell integrity signaling and response to stress in fission yeast. *Curr. Protein Pept. Sci.* **11**, 680-692
7. Arellano, M., Valdivieso, M., Calonge, T., Coll, P., Duran, A., and Perez, P. (1999) *Schizosaccharomyces pombe* protein kinase C homologues, pck1p and pck2p, are targets of rho1p and rho2p and differentially regulate cell integrity. *J. Cell Sci.* **112**, 3569-3578
8. Villar-Tajadura, M., Coll, P., Madrid, M., Cansado, J., Santos, B., and Perez, P. (2008) Rga2 is a Rho2 GAP that regulates morphogenesis and cell integrity in *S. pombe*. *Mol. Microbiol.* **70**, 867-881
9. Mukai, H. (2003) The structure and function of PKN, a protein kinase having a catalytic domain homologous to that of PKC. *J. Biochem.* **133**, 17-27
10. Calonge, T., Nakano, K., Arellano, M., Arai, R., Katayama, S., Toda, T., Mabuchi, I., and Perez, P. (2000) *Schizosaccharomyces pombe* Rho2p GTPase regulates cell wall alpha-glucan biosynthesis through the protein kinase Pck2p. *Mol. Biol. Cell* **11**, 4393-4401
11. Madrid, M., Soto, T., Khong, H., Franco, A., Vicente, J., Perez, P., Gacto, M., and Cansado, J. (2006) Stress-induced response, localization, and regulation of the Pmk1 cell integrity pathway in *Schizosaccharomyces pombe*. *J. Biol. Chem.* **281**, 2033-2043

12. Sanchez-Mir, L., Soto, T., Franco, A., Madrid, M., Viana, R. A., Vicente, J., Gacto, M., Perez, P., and Cansado, J. (2014) Rho1 GTPase and PKC ortholog Pck1 are upstream activators of the cell integrity MAPK pathway in fission yeast. *PLoS One* **9**, e88020
13. Madrid, M., Fernandez-Zapata, J., Sanchez-Mir, L., Soto, T., Franco, A., Vicente-Soler, J., Gacto, M., and Cansado, J. (2013) Role of the fission yeast cell integrity MAPK pathway in response to glucose limitation. *BMC Microbiol.* **13**, 34
14. Madrid, M., Jimenez, R., Sanchez-Mir, L., Soto, T., Franco, A., Vicente-Soler, J., Gacto, M., Perez, P., and Cansado, J. (2015) Multiple layers of regulation influence cell integrity control by the PKC ortholog Pck2 in fission yeast. *J. Cell Sci.* **128**, 266-280
15. Madrid, M., Vazquez-Marin, B., Franco, A., Soto, T., Vicente-Soler, J., Gacto, M., and Cansado, J. (2016) Multiple crosstalk between TOR and the cell integrity MAPK signaling pathway in fission yeast. *Sci. Rep.* **6**, 37515
16. Barba, G., Soto, T., Madrid, M., Nunez, A., Vicente, J., Gacto, M., and Cansado, J. (2008) Activation of the cell integrity pathway is channelled through diverse signalling elements in fission yeast. *Cell. Signal.* **20**, 748-757
17. Graub, R., Hilti, N., Niederberger, C., and Schweingruber, M. (2003) Ksg1, a homologue of the phosphoinositide-dependent protein kinase 1, controls cell wall integrity in *Schizosaccharomyces pombe*. *J. Basic Microbiol.* **43**, 473-482
18. Carpy, A., Krug, K., Graf, S., Koch, A., Popic, S., Hauf, S., and Macek, B. (2014) Absolute proteome and phosphoproteome dynamics during the cell cycle of *Schizosaccharomyces pombe* (fission yeast). *Mol. Cell. Proteomics* **13**, 1925-1936
19. Ma, Y., Kuno, T., Kita, A., Asayama, Y., and Sugiura, R. (2006) Rho2 is a target of the farnesyltransferase Cpp1 and acts upstream of Pmk1 mitogen-activated protein kinase signaling in fission yeast. *Mol. Biol. Cell* **17**, 5028-5037
20. Gould, C. M., Antal, C. E., Reyes, G., Kunkel, M. T., Adams, R. A., Ziyar, A., Riveros, T., and Newton, A. C. (2011) Active site inhibitors protect protein kinase C from dephosphorylation and stabilize its mature form. *J. Biol. Chem.* **286**, 28922-28930
21. Pears, C. J., Kour, G., House, C., Kemp, B. E., and Parker, P. J. (1990) Mutagenesis of the pseudosubstrate site of protein kinase C leads to activation. *Eur. J. Biochem.* **194**, 89-94
22. Lu, Z., and Hunter, T. (2009) Degradation of activated protein kinases by ubiquitination. *Annu. Rev. Biochem.* **78**, 435-475
23. Sugiura, R., Toda, T., Shuntoh, H., Yanagida, M., and Kuno, T. (1998) pmp1(+), a suppressor of calcineurin deficiency, encodes a novel MAP kinase phosphatase in fission yeast. *EMBO J.* **17**, 140-148
24. Viana, R. A., Pinar, M., Soto, T., Coll, P. M., Cansado, J., and Perez, P. (2013) Negative functional interaction between cell integrity MAPK pathway and Rho1 GTPase in fission yeast. *Genetics* **195**, 421-432
25. Cameron, A. J., Escribano, C., Saurin, A. T., Kostelecky, B., and Parker, P. J. (2009) PKC maturation is promoted by nucleotide pocket occupation independently of intrinsic kinase activity. *Nat. Struct. Mol. Biol.* **16**, 624-630

26. Liu, Y., Belkina, N., Graham, C., and Shaw, S. (2006) Independence of protein kinase C-delta activity from activation loop phosphorylation - Structural basis and altered functions in cells. *J. Biol. Chem.* **281**, 12102-12111
27. Wang, Y., Zhang, H., Gao, Y., Huang, C., Zhou, A., Zhou, Y., and Li, Y. (2016) Sequential posttranslational modifications regulate PKC degradation. *Mol. Biol. Cell.* **27**, 410-420
28. Antal, C. E., and Newton, A. C. (2014) Tuning the signalling output of protein kinase C. *Biochem. Soc. Trans.* **42**, 1477-1483
29. Moreno, S., Klar, A., and Nurse, P. (1991) Molecular genetic-analysis of fission yeast *Schizosaccharomyces pombe*. *Method. Enzymol.* **194**, 795-823
30. Guan, K., and Dixon, J. (1991) Eukaryotic proteins expressed in *Escherichia coli*: an improved thrombin cleavage and purification procedure of fusion proteins with glutathione S-transferase. *Anal. Biochem.* **192**, 262-267
31. Takada, H., Nishimura, M., Asayama, Y., Mannse, Y., Ishiwata, S., Kita, A., Doi, A., Nishida, A., Kai, N., Moriuchi, S., Tohda, H., Giga-Hama, Y., Kuno, T., and Sugiura, R. (2007) Atf1 is a target of the mitogen-activated protein kinase Pmk1 and regulates cell integrity in fission yeast. *Mol. Biol. Cell* **18**, 4794-4802
32. Schneider, C., Rasband, W., and Eliceiri, K. (2012) NIH Image to ImageJ: 25 years of image analysis. *Nat. Methods* **9**, 671-675

FOOTNOTES

This work was supported by the Ministerio de Economía y Competitividad grants BFU2014-52828-P, and BIO2015-69958-P, and the Fundación Séneca grant 19246/PI/14, Spain. European Regional Development Fund (ERDF) co-funding from the European Union.

FIGURE LEGENDS

FIGURE 1. *A*, Domain structure of PKC orthologs Pkc1 (*S. cerevisiae*), and Pck1 and Pck2 (*S. pombe*). Labels: HR1, putative rho-binding repeat; C2, putative Ca(2+)-binding motif; Ps, putative pesudosubstrate motif; C1, putative diacylglycerol binding motif. Amino acid sequence alignment of Pck1 and Pck2 catalytic domains is also shown. Conserved canonical phosphorylated residues within AL, TM, and HM are marked with asterisks. *B*, The cell integrity MAPK pathway in *S. pombe*.
The thickness of the solid arrows denotes the relevance of each cascade component during downstream signaling to the MAPK module. For a detailed description of the pathway, please see text.

FIGURE 2. Pck1 is phosphorylated in vivo within AL at T823 by Ksg1, and is more stable than the Pck2 isoform. *A,* GST:*pck1* (control) and GST:*pck1-T823A* fusions were incubated at 30ºC for 1 h with either GST:*ksg1-KD* (kinase dead mutant) or GST:*ksg1* with/without ATP. Reaction mixtures were resolved and hybridized with anti-phospho-T823 or anti-GST antibodies. Results representative of two independent experiments are shown. *B,* Strains MM1578 (*pck1:HA*; Control) and MM1724 (*pck1:HA Ksg1-208*) were grown at 25ºC in YES medium and then incubated at 36ºC for the indicated times. Cell extracts were resolved by SDS-PAGE and hybridized with anti-phospho T823 and anti-HA antibodies. Relative units for total (gray bars) and T-823 phosphorylated (black bars) Pck1 levels were estimated with respect to the internal control (anti-cdc2 blot) at each time point. Results representative

of two independent experiments are shown. *C*, Growing cultures of strains MM1578 (*pck1:HA;* control) and MM1718 (*tor1Δ pck1:HA*) were treated with either 0.6 M KCl, 1 μg/ml Caspofungin, or shifted to the same medium without glucose and supplemented with 3% glycerol. Cell extracts were resolved by SDS-PAGE and hybridized separately with anti-phospho T823 and anti-HA antibodies. Relative units as mean ± SD (biological triplicates) for total (gray bars) and T-823 phosphorylated (black bars) Pck1 levels were estimated as above. *, $P<0.05$; **, $P<0.005$, as calculated by unpaired Student´s *t* test. *D*, Total (anti-HA) Pck1 and Pck2 levels were determined in growing cultures of control strains MM913 (*pck2:HA*) and MM1578 (*pck1:HA*), and after treatment with 0.6 M KCl for 30 min. Relative units as mean ± SD (biological triplicates) for total Pck1 and Pck2 levels were estimated with respect to the internal control (anti-cdc2 blot). **, $P<0.005$, as calculated by unpaired Student´s *t* test. *E*, Control strains MM913 and MM1578 were grown to early-log phase and incubated with or without 100 μg/ml cycloheximide for the indicated times. Cell extracts were hybridized with anti-HA antibodies. Relative units for total Pck1 and Pck2 levels were estimated with respect to the internal control (anti-cdc2 blot) at each time point. Results representative of two independent experiments are shown.

FIGURE 3. Putative in vivo phosphorylation within AL, TM and HM sites is essential for protein stability and biological functions of Pck1, but not Pck2. *A*, Both total (anti-HA) and T-842 phosphorylated (anti-phospho T842 antibody) Pck2 levels were detected in strains expressing *pck2:HA* versions with the indicated mutations. Relative units as mean ± SD (biological duplicates) for total (gray bars) and T-842 phosphorylated (black bars) Pck2 levels were determined with respect to the internal control (anti-cdc2 blot) at each time point. *B*, Total (anti-HA) and T-823 phosphorylated (anti-phospho T823 antibody) Pck1 levels were detected in strains expressing *pck1:HA* versions with the indicated mutations. Relative units as mean ± SD (biological duplicates) for total (gray bars) and T-842 phosphorylated (black bars) Pck2 levels were determined with respect to the internal control as in (*A*). *C*, Serially diluted cells of strains with the indicated genotypes were spotted on YES plates supplemented with either 1 μg/ml Caspofungin, 100 μg/ml Calcofluor white, or 0.1 M $MgCl_2$, and incubated for 3 days at 28ºC. Results representative of three independent experiments are shown. *D*, *Upper panel*: Strains GB35 (*pck1::ura4*$^+$ *pmk1:HA6H*) and GB3 (*pck2::kanR pmk1:HA6H*) were separately transformed with plasmids pREP3X-*pck1:HA* (Control), pREP3X-*pck1-T823A:HA*, pREP3X-*pck2:HA* (Control), and pREP3X-*pck2-T842A:HA*. Serially diluted cells from the above transformants were spotted on EMM2 plates with or without 5 mM thiamine, and incubated for 4 days at 28°C. Results representative of three independent experiments are shown. *Lower panel*: Cell morphology of a transformant expressing pREP3X-*pck1-T823A:HA* plasmid growing in the presence or absence of thiamine (18 hours), was analyzed by fluorescence microscopy after staining with Calcofluor white. *E*, Strains MM1578 (*pck1:HA;* control) and MM1688 (*pck1-T823A:HA*), expressing a genomic *pmk1:HA6H* fusion, were grown in YES medium and treated with 0.6 M KCl. Aliquots were harvested at the times indicated and activated/total Pmk1 were detected with anti-phosho-p44/42 and anti-HA antibodies, respectively. Relative units as mean ± SD (biological triplicates) for Pmk1 activation (anti-phosho-p44/42 blot) were determined with respect to the internal control (anti-HA blot) at each time point.*, $P<0.05$, as calculated by unpaired Student´s *t* test. *F*, Serially diluted cells of strains with the indicated genotypes were spotted on YES plates supplemented with either 1.2 μg/ml

Caspofungin, 100 μg/ml Calcofluor white, or 0.1 M $MgCl_2$, and incubated for 3 days at 28ºC. Results representative of three independent experiments are shown.

FIGURE 4. Constitutive activation promotes dephosphorylation and destabilization of Pck2 and altered downstream signaling to the CIP. *A*, Amino acid sequence alignment of pseudosubstrate motif present in human PKCα, and fission yeast Pck1 and Pck2. The conserved alanine residue within the motif is marked with an asterisk. *B*, Cell extracts from growing cultures of strains MM913 (*pck2:HA*; control) and BV813 (*pck2-A392E:HA*) were resolved by SDS-PAGE and hybridized separately with anti-phospho T842 and anti-HA antibodies. Relative units as mean ± SD (biological triplicates) for total (gray bars) and T-842 phosphorylated (black bars) Pck2 levels were determined with respect to the internal control (anti-Pmk1-HA blot). *, $P<0.05$, as calculated by unpaired Student´s *t* test. *C*, Strains MM913 (*pck2:HA;* control), GB3 (*pck2Δ*), and BV813 (*pck2-A392E:HA*), expressing a genomic *pmk1:HA6H* fusion were grown in YES medium, and activated/total Pmk1 were detected with anti-phosho-p44/42 and anti-HA antibodies, respectively. Relative units as mean ± SD (biological triplicates) for Pmk1 phosphorylation (anti-phosho-p44/42 blot) were determined with respect to the internal control (anti-HA blot). *, $P<0.05$; **, $P<0.005$, as calculated by unpaired Student´s *t* test. *D*, Serially diluted cells of strains described in (*C*) were spotted on YES plates supplemented with 0.1 M $MgCl_2$ and incubated for 3 days at 28ºC. Results representative of three independent experiments are shown. *E*, Growing strains described in (*B*) were treated with either 1 μg/ml Caspofungin or 0.6 M KCl. Total Pck2 levels were detected after incubation with anti-HA antibodies. Anti-cdc2 was used as loading control. Results representative of two independent experiments are shown. *F*, Strains described in (*B*) were treated with either 1 μg/ml Caspofungin or 0.6 M KCl and activated/total Pmk1 was detected as above. Relative units for Pmk1 phosphorylation (anti-phosho-p44/42 blot) were determined with respect to the internal control (anti-HA blot). Results representative of two independent experiments are shown.

FIGURE 5. Constitutive catalytic activation stabilizes Pck1 and interferes with proper downstream signaling to the CIP triggered by Pck2. *A*, Cell extracts from growing cultures of strains MM1578 (*pck1:HA;* control) and MM1746 (*pck1-A399E:HA*) were resolved by SDS-PAGE and hybridized separately with anti-phospho T823 and anti-HA antibodies. Relative units as mean ± SD (biological triplicates) for total (gray bars) and T-823 phosphorylated (black bars) Pck1 levels were determined with respect to the internal control (anti-Pmk1-HA blot). *, $P<0.05$, as calculated by unpaired Student´s *t* test. *B*, Growing cultures of strains MM1578 (*pck1:HA;* control) and MM1746 (*pck1-A399E:HA*) were treated with either 1 μg/ml Caspofungin or 0.6 M KCl. Cell extracts were resolved by SDS-PAGE and hybridized separately with anti-phospho T823 and anti-HA antibodies. Anti-cdc2 was used as loading control. Results representative of two independent experiments are shown. *C*, Strains MM1578 (*pck1:HA;* control), MM2096 (*pck2Δ*), MM1746 (*pck1-A399E:HA*), and BV630 (*pck1-A399E:HA pck2Δ*), expressing genomic *pmk1:HA6H* fusions, were grown in YES medium, and activated/total Pmk1 were detected with anti-phosho-p44/42 and anti-HA antibodies, respectively. Relative units as mean ± SD (biological triplicates) for Pmk1 phosphorylation (anti-phosho-p44/42 blot) were determined with respect to the internal control (anti-HA blot). *, $P<0.05$, as calculated by

unpaired Student´s *t* test. *D*, Serially diluted cells of strains described in (*C*) were spotted on YES plates supplemented with 0.1-0.2 M $MgCl_2$, and incubated for 3 days at 28ºC. Results representative of three independent experiments are shown. *E*, Strains described in (*C*) were grown in YES medium and treated with 0.6 M KCl. Aliquots were harvested at the times indicated and activated/total Pmk1 were detected with anti-phosho-p44/42 and anti-HA antibodies, respectively. Relative units as mean ± SD (biological triplicates) for Pmk1 phosphorylation (anti-phosho-p44/42 blot) were determined with respect to the internal control (anti-HA blot) at each time point. *, $P<0.05$, as calculated by unpaired Student´s *t* test. *F*, Cell morphology of strains MM1578 (*pck1:HA;* control), MM1904 (*pmk1Δ*), MM1746 (*pck1-A399E:HA*), and MM2119 (*pck1-A399E:HA pmk1Δ*), was analyzed by fluorescence microscopy after staining with Calcofluor white. *G*, The percentage of unseptated/septated/multiseptated cells (as mean ± SD; total number of cells ≥400) in exponentially growing cultures of strains described in (*F*), was determined by fluorescence microscopy after cell staining with Calcofluor white. *, $P<0.05$, as calculated by unpaired Student´s *t* test. *H*, Control and *pmk1Δ* strains were separately transformed with plasmids pREP3X-*pck1:HA* (Control) and pREP3X-*pck1-A399E:HA*. Serially diluted cells from the above transformants were spotted on EMM2 plates with or without 5 mM thiamine, and incubated for 4 days at 28°C. Results representative of three independent experiments are shown.

FIGURE 6. Pck1 is the main Rho1 effector during control of cell growth and cell integrity signaling. *A*, Serially diluted cells of strains MM1578 (*pck1:HA;* control), MM1746 (*pck1-A399E:HA*), MM2139 (*pck1:HA rho1-596*), and MM2143 (*pck1-A399E:HA rho1-596*), were spotted on YES plates and incubated for 3 days at 25, 28, 30, 32 and 37ºC (upper panels), and YES plates supplemented with either 0.5 or 1 µg/ml Caspofungin, and incubated for 3 days at 28ºC (lower panels). Results representative of three independent experiments are shown. *B*, Cell morphology of strains MM1746 (*pck1-A399E:HA*) and MM2143 (*pck1-A399E:HA rho1-596*) growing in YES medium was analyzed by fluorescence microscopy after staining with Calcofluor white. *C*, Growing cultures of strains described in (*A*) were treated with 0.6 M KCl for 60 min. Cell extracts were resolved by SDS-PAGE and hybridized separately with anti-phospho T823 and anti-HA antibodies. Anti-cdc2 was used as loading control. Results representative of two independent experiments are shown. *D*, Strains described in (*A*) and expressing a genomic Pmk1-HA6H fusion were grown in YES medium, and activated/total Pmk1 were detected with anti-phosho-p44/42 and anti-HA antibodies, respectively. Relative units as mean ± SD (biological triplicates) for Pmk1 phosphorylation (anti-phosho-p44/42 blot), were determined with respect to the internal control (anti-HA blot). *, $P<0.05$, as calculated by unpaired Student´s *t* test. *E*, Strains MM1578 (*pck1:HA;* control), MM1746 (*pck1-A399E:HA*), MM2140 (*pck1:HA rho1-596 rho2Δ*), MM2144 (*pck1-A399E:HA rho1-596 rho2Δ*), MM2135 (*pck1:HA rho2Δ*), and MM2183 (*pck1-A399E:HA rho2Δ*), expressing genomic *pmk1:HA6H* fusions, were grown in YES medium, and activated/total Pmk1 were detected with anti-phosho-p44/42 and anti-HA antibodies, respectively. Relative units as mean ± SD (biological triplicates) for Pmk1 phosphorylation (anti-phosho-p44/42 blot) were determined with respect to the internal control (anti-HA blot). *, $P<0.05$, as calculated by unpaired Student´s *t* test.

FIGURE 7. Catalytic activity is essential for Pck1 functions, while Pck2 remains partially functional in absence of intrinsic kinase activity. *A*, Amino acid sequence alignment of ATP catalytic region present in human PKCα, and fission yeast Pck1 and Pck2. The conserved catalytic aspartic acid residue within the motif is marked with an asterisk. *B*, Cell extracts from growing cultures of strains MM913 (*pck2:HA;* control), BV813 (*pck2-A392E:HA*), BV623 (*pck2-D808N:HA*), and BV625 (*pck2-A392E D808N:HA*), were resolved by SDS-PAGE and hybridized separately with anti-phospho T842 and anti-HA antibodies. Relative units as mean ± SD (biological triplicates) for total (gray bars) and T-842 phosphorylated (black bars) Pck2 levels were determined with respect to the internal control (anti-cdc2 blot). *, $P<0.05$, as calculated by unpaired Student´s *t* test. *C*, Strains described in (*B*) and expressing a genomic *pmk1:HA6H* fusion were grown in YES medium, and activated/total Pmk1 were detected with anti-phosho-p44/42 and anti-HA antibodies, respectively. Relative units as mean ± SD (biological triplicates) for Pmk1 phosphorylation (anti-phosho-p44/42 blot), were determined with respect to the internal control (anti-HA blot). *, $P<0.05$; **, $P<0.005$, as calculated by unpaired Student´s *t* test. *D*, Strains described in (*B*) were grown in YES medium and treated with 0.6 M KCl. Aliquots were harvested at the times indicated and activated/total Pmk1 were as above. Relative units for Pmk1 phosphorylation (anti-phosho-p44/42 blot) were determined with respect to the internal control (anti-HA blot) at each time point. Results representative of three independent experiments are shown. *E*, Cell extracts from growing cultures of strains MM1578 (*pck1:HA;* control), MM1746 (*pck1-A399E:HA*), BV627 (*pck1-D789N:HA*), and BV629 (*pck1-A399E D789N:HA*), were resolved by SDS-PAGE and hybridized separately with anti-phospho T823 and anti-HA antibodies. Relative units as mean ± SD (biological triplicates) for total (gray bars) and T-823 phosphorylated (black bars) Pck1 levels were determined with respect to the internal control (anti-cdc2 blot).*, $P<0.05$, as calculated by unpaired Student´s *t* test. *F*, Strains described in (*E*) and expressing a genomic *pmk1:HA6H* fusion were grown in YES medium, and activated/total Pmk1 were detected as above. Relative units as mean ± SD (biological triplicates) for Pmk1 phosphorylation (anti-phosho-p44/42 blot), were determined with respect to the internal control (anti-HA blot). **, $P<0.005$, as calculated by unpaired Student´s *t* test. *G*, Cell morphology of strains MM1746 (*pck1-A399E:HA*) and BV629 (*pck1-A399E D789N:HA*) was analyzed by fluorescence microscopy after staining with Calcofluor white. *H*, Serially diluted cells of strains GB35 (*pck1Δ*) plus those described in (*F*) were spotted on YES plates supplemented with 0.8-1.2-1.5 μg/ml Caspofungin, and incubated for 3 days at 28ºC. Results representative of three independent experiments are shown. *I*, Serially diluted cells of strains GB3 (*pck2Δ*) plus those described in (*B*) were spotted on YES plates supplemented with 1-1.2 μg/ml Caspofungin, and incubated for 3 days at 28ºC. Results representative of three independent experiments are shown.

FIGURE 8. Proposed model for differential functional regulation of fission yeast PKC orthologs Pck1 and Pck2. *A*, Once synthesized, highly unstable Pck1 must be phosphorylated in vivo within AL by Ksg1 (PDK) to promote kinase stabilization and biological functions. *B*, Contrariwise, Pck2 exists as a mixture of AL-phosphorylated and -unphosphorylated isoforms, since AL-unphosphorylated Pck2 is stable and is partially functional (+) in the absence of kinase activity. Both kinases become fully phosphorylated within the catalytic domain to adopt a mature and primed conformation (+++); however, whereas activated Pck2 is prone to rapid degradation, active Pck1 remains stable and functional for longer times. Differential regulation of stability and function of both kinase isoforms

may allow for a graded and flexible control of their shared and specific downstream signaling functions.

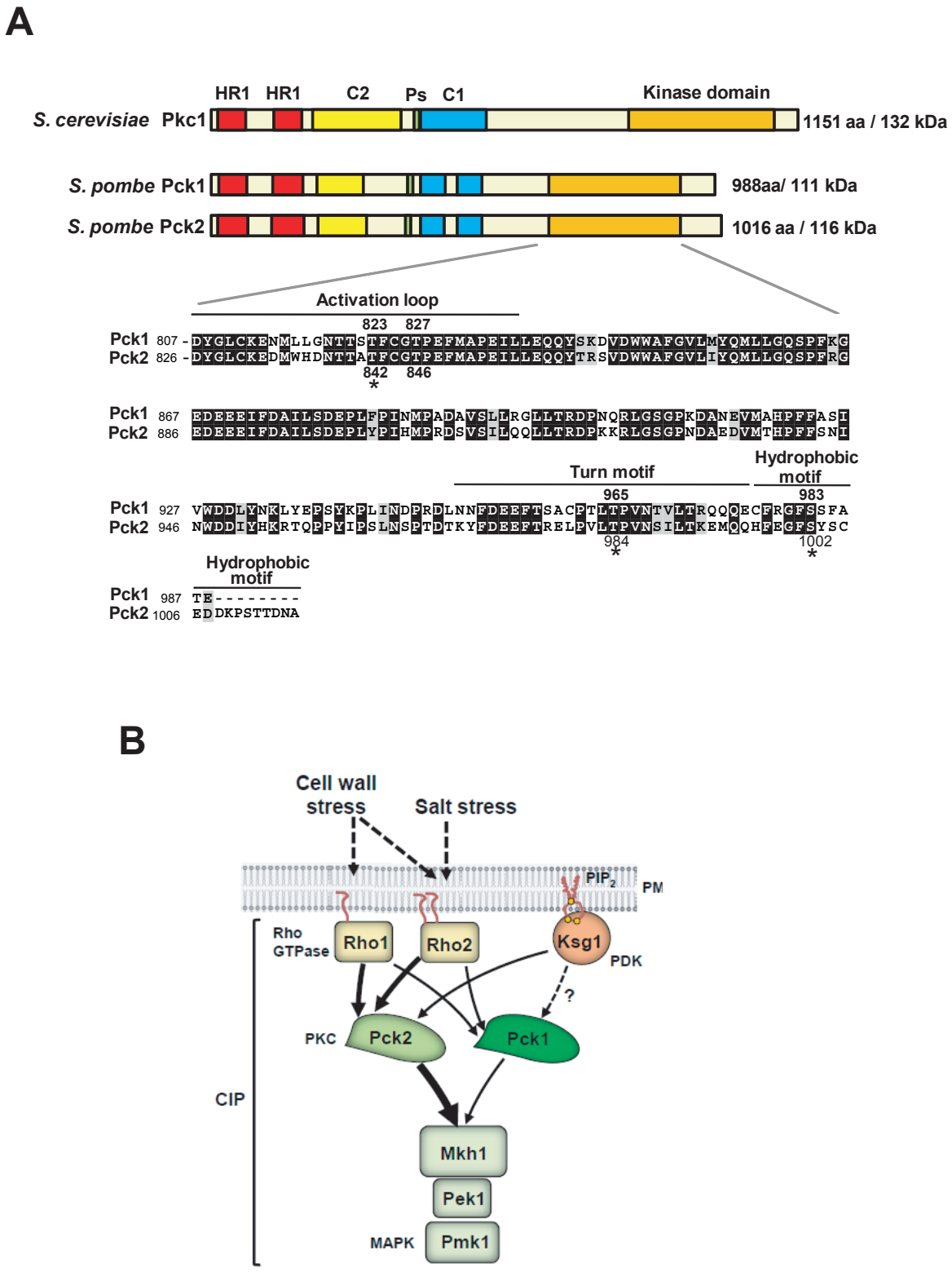
A
HR1 HR1 C2 Ps C1 Kinase domain
S. cerevisiae Pkc1
1151 aa / 132 kDa
S. pombe Pck1
988aa/ 111 kDa
S. pombe Pck2
1016 aa / 116 kDa
Activation loop
823 827
Pck1 807 -DYGLCKENMLLGNTTSTFCGTPEFMAPEILLEQQYSKDVDWWAFGVLMYQMLLGQSPFKG
Pck2 826 -DYGLCKEDMWHDNTTATFCGTPEFMAPEILLEQQYTRSVDWWAFGVLIYQMLLGQSPFRG
842 846
Pck1 867 EDEEEIFDAILSDEPLFPINMPADAVSLLRGLLTRDPNQRLGSGPKDANEVMAHPFFASI
Pck2 886 EDEEEIFDAILSDEPLYPIHMPRDSVSILQQLLTRDPKKRLGSGPNDAEDVMTHPFFSNI
Turn motif
Hydrophobic motif
965 983
Pck1 927 VWDDLYNKLYEPSYKPLINDPRDLNNFDEEFTSACPTLTPVNTVLTRQQQECFRGFSSFA
Pck2 946 NWDDIYHKRTQPPYIPSLNSPTDTKYFDEEFTRELPVLTPVNSILTKEMQQHFEGFSYSC
984 1002
Hydrophobic motif
Pck1 987 TE--------
Pck2 1006 EDDKPSTTDNA
B
Cell wall stress
Salt stress
PIP2
PM
Rho GTPase
Rho1
Rho2
Ksg1
PDK
?
PKC
Pck2
Pck1
CIP
Mkh1
Pek1
MAPK
Pmk1

Figure 1

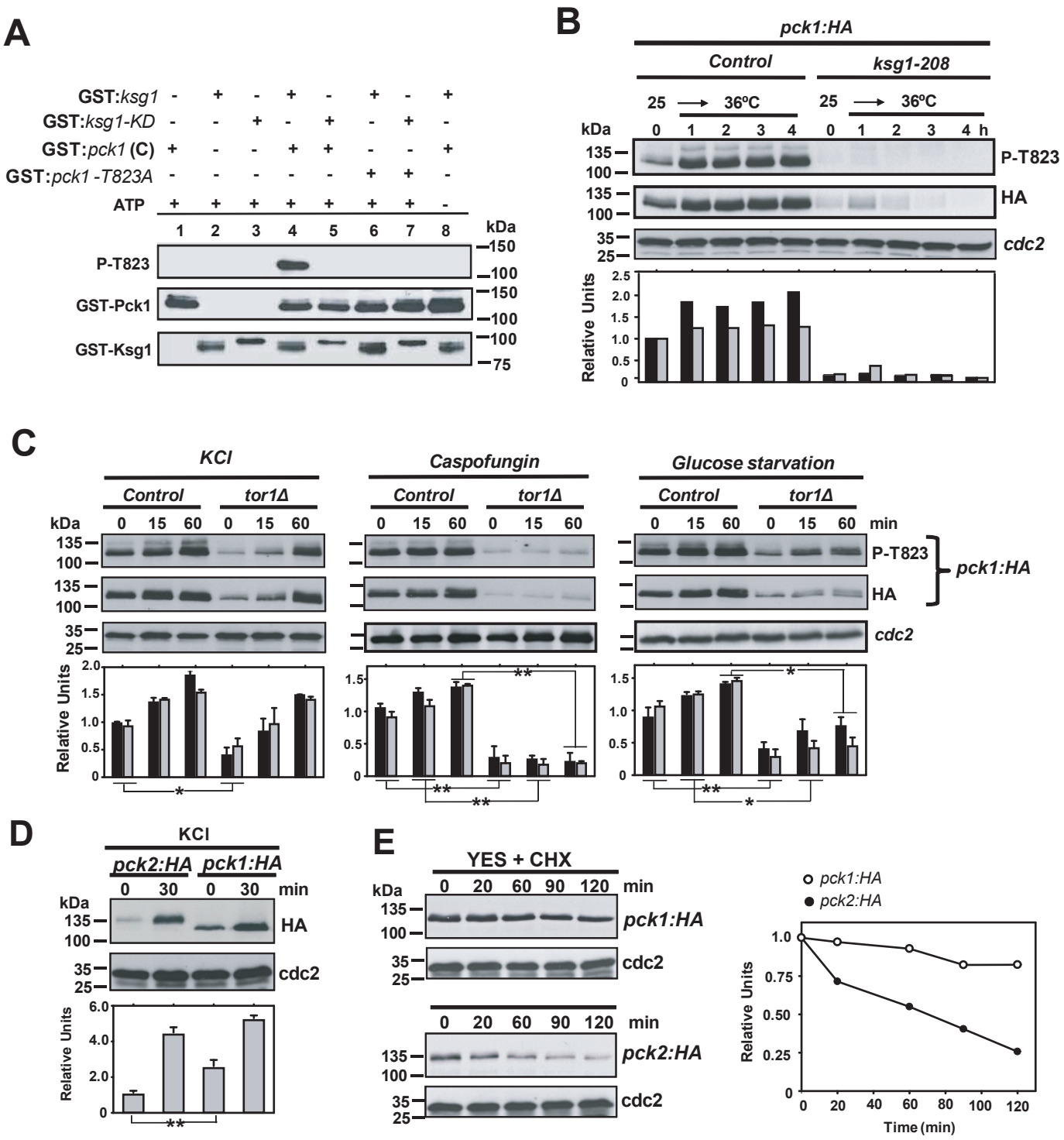
A
GST:ksg1
GST:ksg1-KD
GST:pck1 (C)
GST:pck1 -T823A
ATP
1 2 3 4 5 6 7 8
kDa
P-T823
GST-Pck1
GST-Ksg1
150
100
150
100
100
75
B
pck1:HA
Control
ksg1-208
25 → 36ºC
kDa
0 1 2 3 4 0 1 2 3 4 h
P-T823
HA
cdc2
Relative Units
C
KCl
Caspofungin
Glucose starvation
Control
tor1Δ
kDa
0 15 60 0 15 60 min
P-T823
HA
cdc2
pck1:HA
Relative Units
D
KCl
pck2:HA
pck1:HA
0 30 0 30 min
kDa
HA
cdc2
Relative Units
E
YES + CHX
kDa
0 20 60 90 120 min
pck1:HA
cdc2
pck2:HA
pck1:HA
pck2:HA
Relative Units
Time (min)

Figure 2

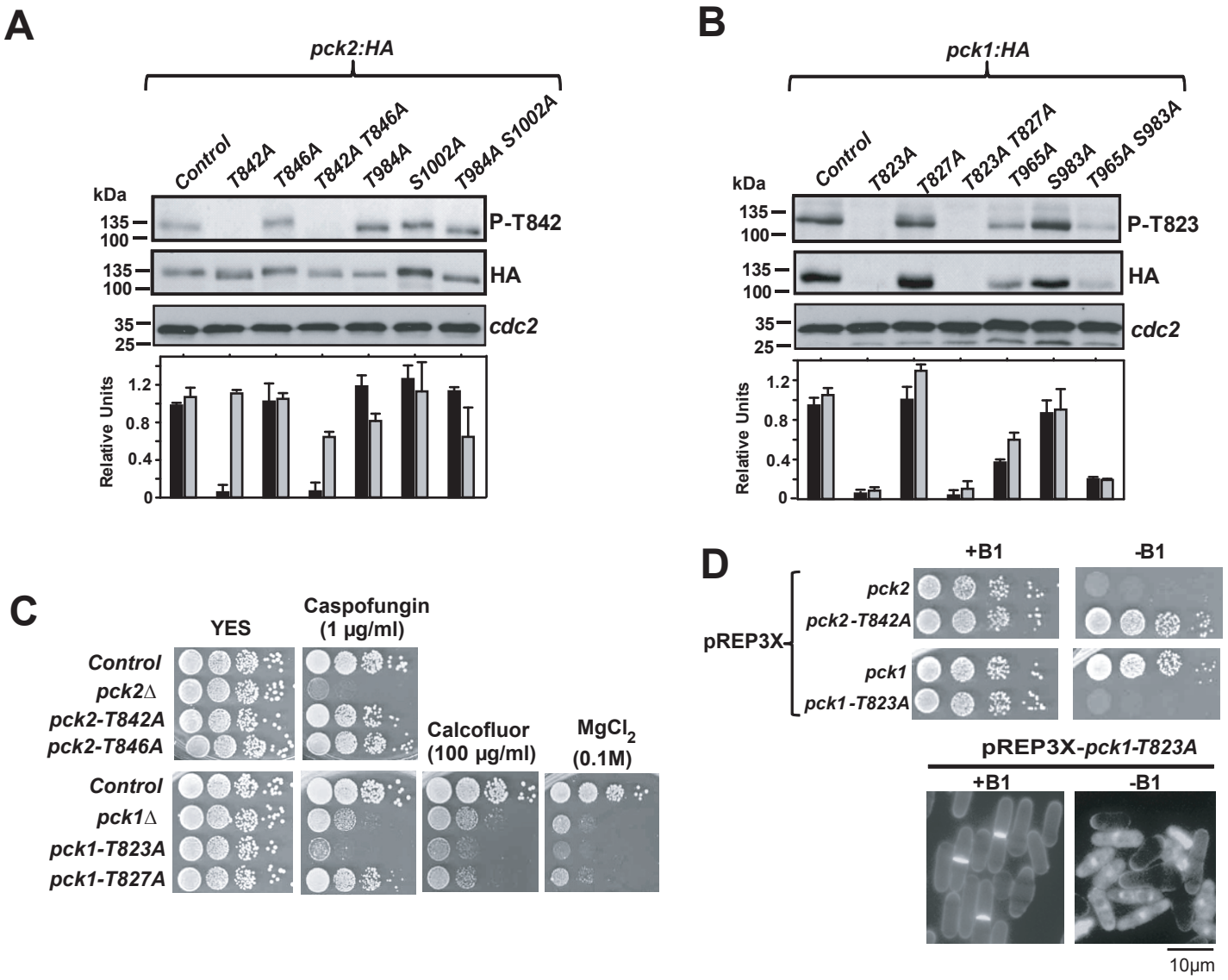
A
pck2:HA
Control
T842A
T846A
T842A T846A
T984A
S1002A
T984A S1002A
kDa
135
100
P-T842
HA
35
25
cdc2
Relative Units
1.2
0.8
0.4
0
B
pck1:HA
Control
T823A
T827A
T823A T827A
T965A
S983A
T965A S983A
P-T823
C
YES
Caspofungin
(1 µg/ml)
Control
pck2Δ
pck2-T842A
pck2-T846A
Calcofluor
(100 µg/ml)
MgCl2
(0.1M)
Control
pck1Δ
pck1-T823A
pck1-T827A
D
+B1
-B1
pREP3X
pck2
pck2-T842A
pck1
pck1-T823A
pREP3X-pck1-T823A
10µm
E
KCl
Control
pck1-T823A
0
15
30
60
90
min
P-p44/42
F
YES
Caspofungin
(1.2 µg/ml)
Control
pck2Δ
pck2-T984A
pck2-S1002A
pck2-T984A
S1002A
Calcofluor
(100 µg/ml)
MgCl2
(0.1M)
Control
pck1Δ
pck1-T965A
pck1-S983A
pck1-T965A
S983A

Figure 3

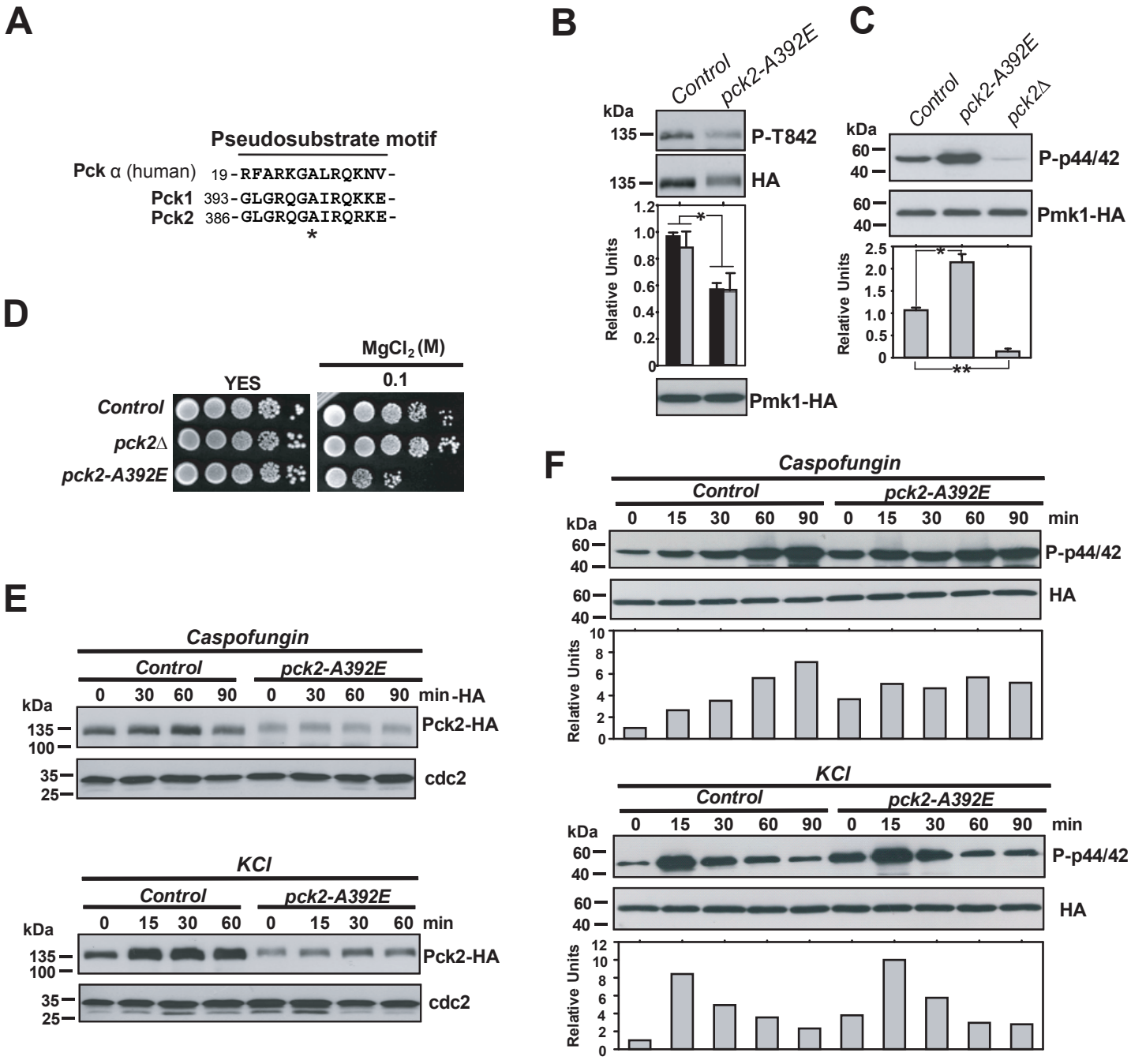
A
Pseudosubstrate motif
Pck α (human) 19-RFARKGALRQKNV-
Pck1 393-GLGRQGAIRQKKE-
Pck2 386-GLGRQGAIRQRKE-
*
B
Control
pck2-A392E
kDa
135
P-T842
135
HA
Relative Units
Pmk1-HA
C
Control
pck2-A392E
pck2Δ
kDa
60
40
P-p44/42
Pmk1-HA
Relative Units
D
MgCl2 (M)
YES
0.1
Control
pck2Δ
pck2-A392E
E
Caspofungin
Control
pck2-A392E
0 30 60 90 0 30 60 90 min
kDa
135
100
Pck2-HA
35
25
cdc2
KCl
Control
pck2-A392E
0 15 30 60 0 15 30 60 min
Pck2-HA
cdc2
F
Caspofungin
Control
pck2-A392E
0 15 30 60 90 0 15 30 60 90 min
kDa
P-p44/42
HA
Relative Units
KCl
Control
pck2-A392E
0 15 30 60 90 0 15 30 60 90 min
P-p44/42
HA
Relative Units

Figure 4

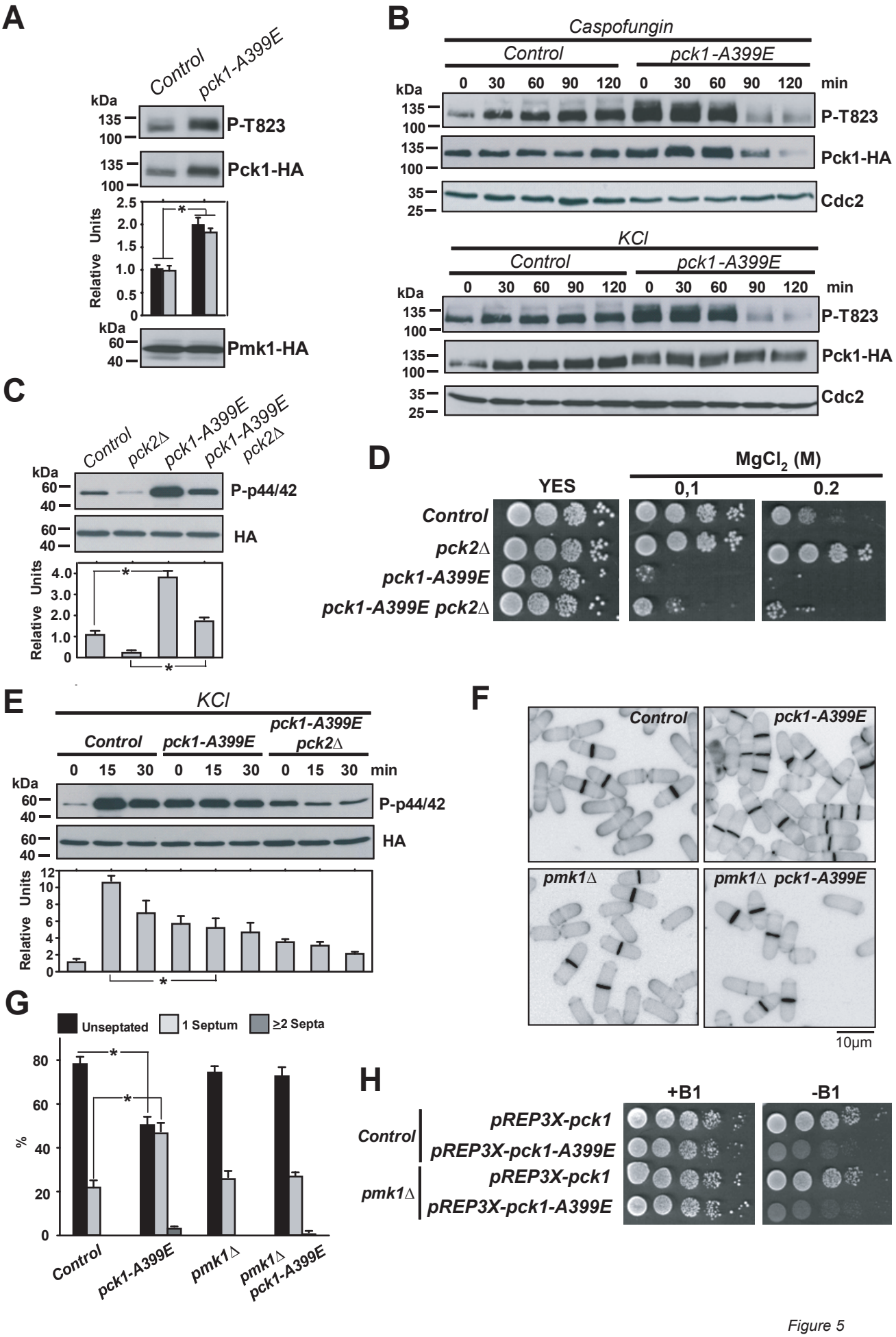
A
Control
pck1-A399E
kDa
135
100
P-T823
135
100
Pck1-HA
Relative Units
2.5
2.0
1.5
1.0
0.5
0
*
kDa
60
40
Pmk1-HA
B
Caspofungin
Control
pck1-A399E
0 30 60 90 120 0 30 60 90 120 min
kDa
135
100
P-T823
135
100
Pck1-HA
35
25
Cdc2
KCl
Control
pck1-A399E
0 30 60 90 120 0 30 60 90 120 min
kDa
135
100
P-T823
135
100
Pck1-HA
35
25
Cdc2
C
Control
pck2Δ
pck1-A399E
pck1-A399E pck2Δ
kDa
60
40
P-p44/42
60
40
HA
Relative Units
4.0
3.0
2.0
1.0
0
*
*
D
MgCl2 (M)
YES
0,1
0.2
Control
pck2Δ
pck1-A399E
pck1-A399E pck2Δ
E
KCl
Control
pck1-A399E
pck1-A399E pck2Δ
0 15 30 0 15 30 0 15 30 min
kDa
60
40
P-p44/42
60
40
HA
Relative Units
12
10
8
6
4
2
0
*
F
Control
pck1-A399E
pmk1Δ
pmk1Δ pck1-A399E
10μm
G
Unseptated
1 Septum
≥2 Septa
%
80
60
40
20
0
*
*
Control
pck1-A399E
pmk1Δ
pmk1Δ pck1-A399E
H
+B1
-B1
Control
pREP3X-pck1
pREP3X-pck1-A399E
pmk1Δ
pREP3X-pck1
pREP3X-pck1-A399E

Figure 5

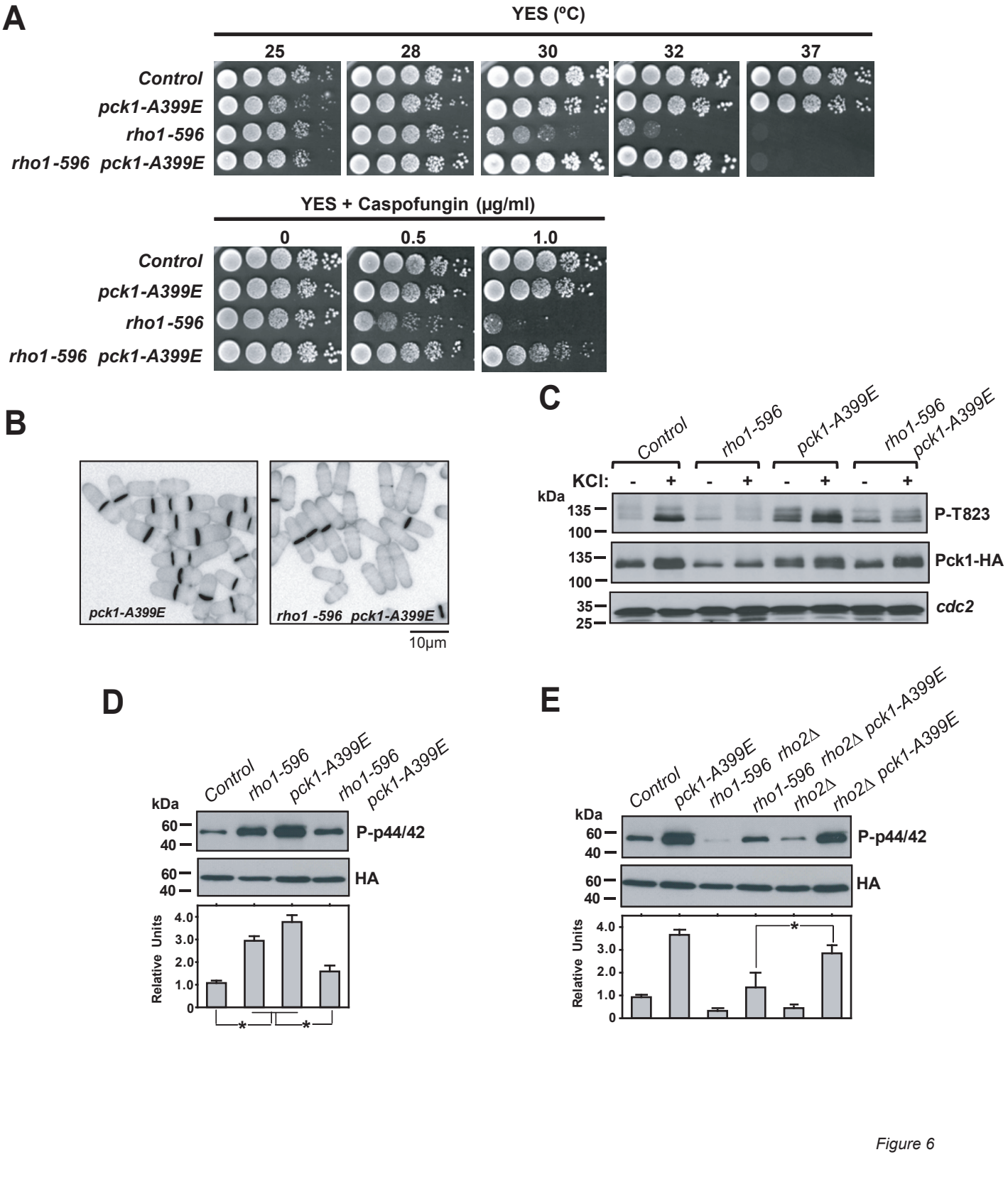
A
YES (ºC)
25
28
30
32
37
Control
pck1-A399E
rho1-596
rho1-596 pck1-A399E
YES + Caspofungin (µg/ml)
0
0.5
1.0
Control
pck1-A399E
rho1-596
rho1-596 pck1-A399E
B
pck1-A399E
rho1 -596 pck1-A399E
10µm
C
Control
rho1-596
pck1-A399E
rho1-596 pck1-A399E
KCl: - + - + - + - +
kDa
135
100
P-T823
135
100
Pck1-HA
35
25
cdc2
D
Control
rho1-596
pck1-A399E
rho1-596
pck1-A399E
kDa
60
40
P-p44/42
60
40
HA
Relative Units
4.0
3.0
2.0
1.0
0
*
*
E
Control
pck1-A399E
rho1-596
rho2Δ
rho1-596 rho2Δ pck1-A399E
rho2Δ
rho2Δ pck1-A399E
kDa
60
40
P-p44/42
60
40
HA
Relative Units
4.0
3.0
2.0
1.0
0
*

Figure 6

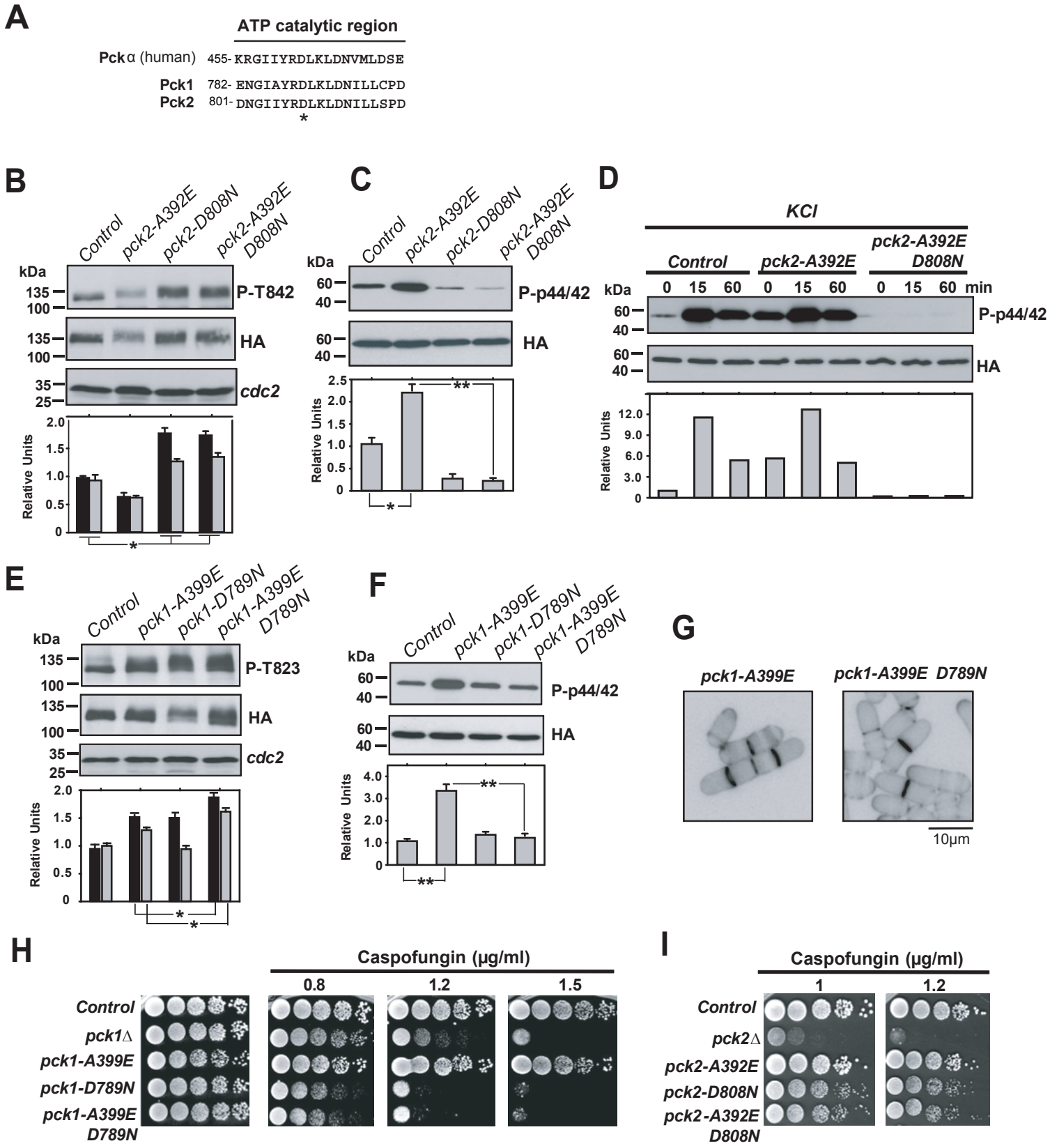
A
ATP catalytic region
Pckα (human) 455- KRGIIYRDLKLDNVMLDSE
Pck1 782- ENGIAYRDLKLDNILLCPD
Pck2 801- DNGIIYRDLKLDNILLSPD
*
B
Control
pck2-A392E
pck2-D808N
pck2-A392E D808N
kDa
135
100
P-T842
HA
35
25
cdc2
Relative Units
C
P-p44/42
HA
D
KCl
Control
pck2-A392E
pck2-A392E D808N
0 15 60 0 15 60 0 15 60 min
P-p44/42
HA
E
pck1-A399E
pck1-D789N
pck1-A399E D789N
P-T823
F
G
pck1-A399E
pck1-A399E D789N
10μm
H
Caspofungin (μg/ml)
0.8
1.2
1.5
Control
pck1Δ
pck1-A399E
pck1-D789N
pck1-A399E D789N
I
1
1.2
pck2Δ
pck2-A392E
pck2-D808N
pck2-A392E D808N

Figure 7

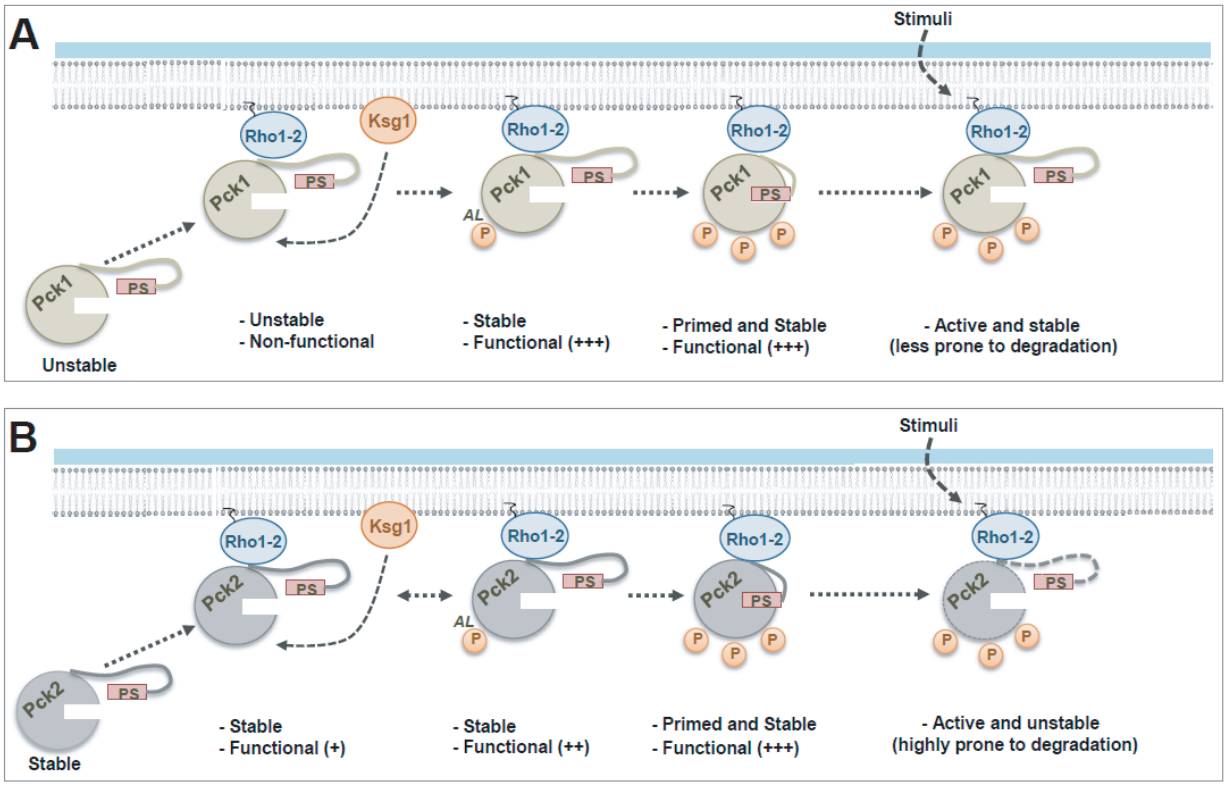
A
Stimuli
Rho1-2
Ksg1
Pck1
PS
AL
P
Unstable
- Unstable
- Non-functional
- Stable
- Functional (+++)
- Primed and Stable
- Functional (+++)
- Active and stable
(less prone to degradation)
B
Stimuli
Rho1-2
Pck2
PS
Stable
- Stable
- Functional (+)
- Stable
- Functional (++)
- Primed and Stable
- Functional (+++)
- Active and unstable
(highly prone to degradation)

Figure 8

Supplemental Data

Differential Functional Regulation of PKC Orthologs in Fission Yeast

Marisa Madrid[1], Beatriz Vázquez-Marín[1], Teresa Soto[1], Alejandro Franco[1], Elisa Cómez-Gil, Jero Vicente-Soler[1], Mariano Gacto[1], Pilar Pérez[2], and José Cansado[1].

[1] Yeast Physiology Group, Department of Genetics and Microbiology, Facultad de Biología, Universidad de Murcia, 30071 Murcia, Spain.
[2] Instituto de Biología Funcional y Genómica (IBFG), Consejo Superior de Investigaciones Científicas, Universidad de Salamanca, 37007 Salamanca, Spain.

Table of Contents

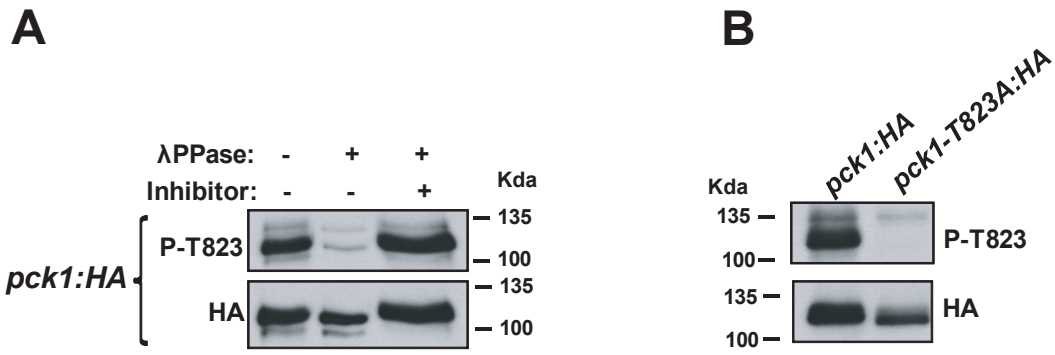

Fig. S1 Validation of Pck1 anti-phospho T823 antibody.
(*A*) Control strain MM1578 (pck1:HA) was grown to early-log phase in YES medium at 28ºC. Cell extracts were prepared and treated with lambda phosphatase in the presence/absence of a specific phosphatase inhibitor. Phosphorylayed and total Pck2 were detected with anti-phospho T823 and anti-HA antibodies, respectively. Results representative of two independent experiments are shown.
(*B*) Strains MM1578 (pck1:HA; control) and MM1688 (pck1-T823A:HA), were grown in YES medium at 28ºC. Cell extracts were resolved by SDS-PAGE and hybridized separately with anti-phospho T823 and anti-HA antibodies. Results representative of two independent experiments are shown.

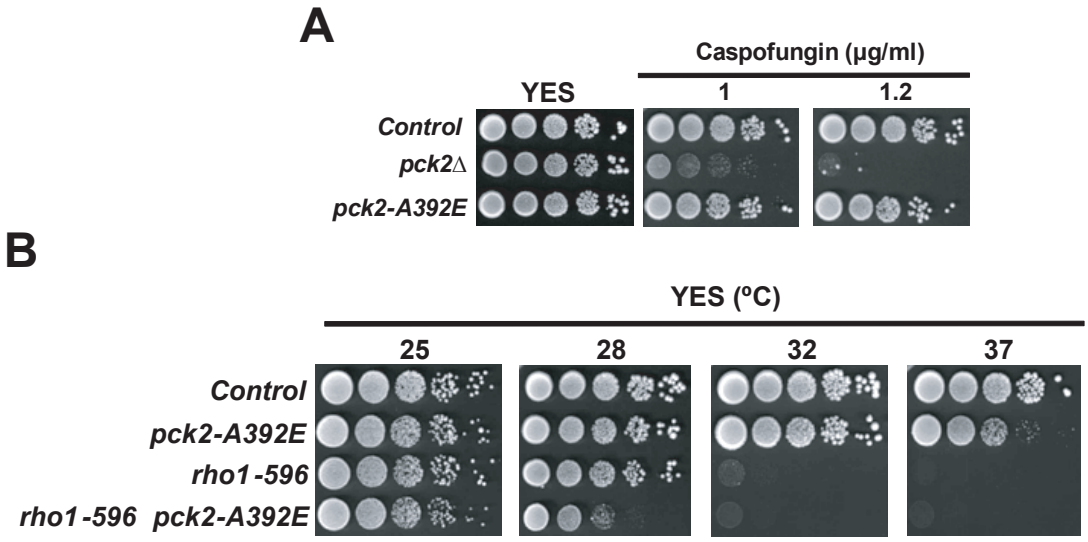

Fig. S2 ***rho1-596*** **thermosensitivity becomes aggravated in the presence of the Pck2-*A392E* pseudosubstrate mutant.**

(*A*) Serially diluted cells of strains MM913 (*pck2:HA;* control), GB3 (*pck2*Δ), and BV813 (*pck2-A392E:HA*), were spotted on YES plates supplemented with 1 or 1.2 µg/ml Caspofungin, and incubated for 3 days at 28ºC. Results representative of three independent experiments are shown.

(*B*)Serially diluted cells of strains MM913(*pck2:HA;* control), BV813 (*pck2-A392E:HA*), BV786 (*pck2:HA rho1-596*), and BV625 (*pck2-A392E:HA rho1- 596*), were spotted on YES plates and incubated for 3 days at 25, 28, 32 and 37ºC. Results representative of three independent experiments are shown.

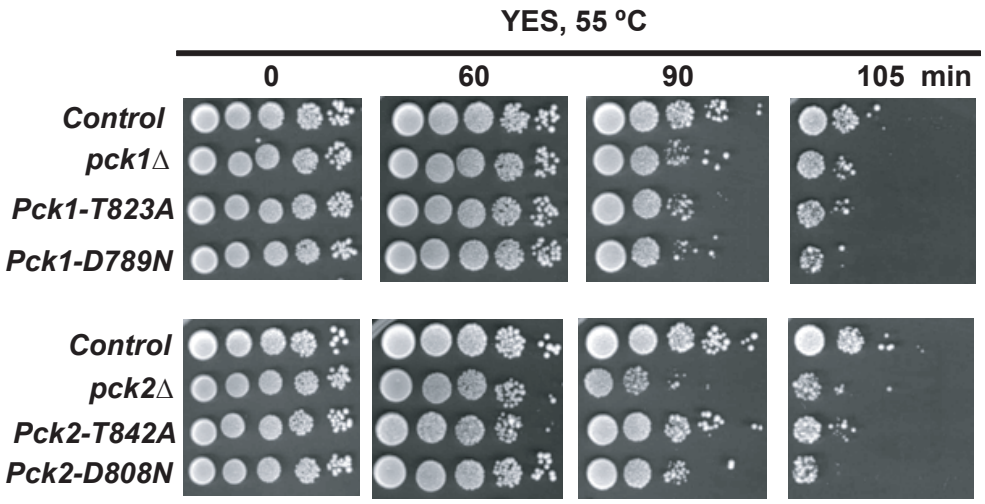

Fig. S3 *pck2*Δ cells exhibit a defective growth recovery phenotype in response to a severe thermal stress.

Serially diluted cells of strains of the indicated genotypes were spotted on YES plates, subjected to a thermal stress at 55ºC for the indicated times, and incubated for 3 days at 28ºC. Results representative of three independent experiments are shown.

Strain	Genotype	Source/Reference
MM1578	*h⁺ pck1::ura pck1-HA:leu1⁺ pmk1-HA6H:ura4⁺*	This work
MM1724	*h? ksg1.208 pck1::ura pck1-HA:leu1⁺ pmk1-HA6H:ura4⁺*	This work
MM1718	*h⁺ tor1Δ pck1::ura pck1-HA:leu1⁺ pmk1-HA6H:ura4⁺*	This work
MM2139	*h? rho1.596:natR pck1::ura pck1-HA:leu1⁺ pmk1-HA6H:ura4⁺*	This work
MM2135	*h? rho2::kanR pck1::ura pck1-HA:leu1⁺ pmk1-HA6H:ura4⁺*	This work
MM1114	*h⁺ pck2::hygR pck2-HA:leu1⁺ pmk1-HA6H:ura4⁺*	This work
BV786	*h? rho1.596:natR pck2::hygR pck2-HA:leu1⁺ pmk1-HA6H:ura4⁺*	This work
BV791	*h? rho2::kanR pck2::hygR pck2-HA:leu1⁺ pmk1-HA6H:ura4⁺*	This work
MM913	*h⁺ pck2::kanR pck2-HA:leu1⁺ pmk1-HA6H:ura4⁺*	Madrid *et al.* (2015)
MM918	*h⁺ pck2::kanR pck2.T842A-HA:leu1⁺ pmk1-HA6H:ura4⁺*	Madrid *et al.* (2015)
MM916	*h⁺ pck2::kanR pck2.T846A-HA:leu1⁺ pmk1-HA6H:ura4⁺*	Madrid *et al.* (2015)
MM921	*h⁺ pck2::kanR pck2.T842AT846A-HA:leu1⁺ pmk1-HA6H:ura4⁺*	Madrid *et al.* (2015)
MM1009	*h⁺ pck2::kanR pck2.T984A-HA:leu1⁺ pmk1-HA6H:ura4⁺*	Madrid *et al.* (2015)
MM1011	*h⁺ pck2::kanR pck2.S1002A-HA:leu1⁺ pmk1-HA6H:ura4⁺*	Madrid *et al.* (2015)
MM1042	*h⁺ pck2::kanR pck2.T984AS1002A-HA:leu1⁺ pmk1-HA6H:ura4⁺*	Madrid *et al.* (2015)
MM1123	*h⁺ pck2::kanR pck2.T842AT984A-HA:leu1⁺ pmk1-HA6H:ura4⁺*	Madrid *et al.* (2015)
MM931	*h⁺ pck2::kanR pck2.T842AT846AT984A-HA:leu1⁺ pmk1-HA6H:ura4⁺*	Madrid *et al.* (2015)
MM1688	*h⁺ pck1::ura pck1.T823A-HA:leu1⁺ pmk1-HA6H:ura4⁺*	This work
MM1734	*h⁺ pck1::ura pck1.T827A-HA:leu1⁺ pmk1-HA6H:ura4⁺*	This work
MM1745	*h⁺ pck1::ura pck1.T823AT827A-HA:leu1⁺ pmk1-HA6H:ura4⁺*	This work
MM1757	*h⁺ pck1::ura pck1.T965A-HA:leu1⁺ pmk1-HA6H:ura4⁺*	This work
MM1761	*h⁺ pck1::ura pck1.S983A-HA:leu1⁺ pmk1-HA6H:ura4⁺*	This work
MM1784	*h⁺ pck1::ura pck1.T965AS983A-HA:leu1⁺ pmk1-HA6H:ura4⁺*	This work
MM1786	*h⁺ pck1::ura pck1.T823AT965A-HA:leu1⁺ pmk1-HA6H:ura4⁺*	This work
MM1789	*h⁺ pck1::ura pck1.T823AT827AT965A-HA:leu1⁺ pmk1-HA6H:ura4⁺*	This work
GB3	*h⁺ pck2::kanR pmk1-HA6H:ura4⁺*	Barba *et al.* (2008)
MM831	*h⁺ pck1::ura⁺ pmk1-HA6H: ura4⁺ pREP3X-pck1⁺*	This work
MM807	*h⁺ pck1::ura⁺ pmk1-HA6H: ura4⁺ pREP3X-pck1.T823A*	This work
MM844	*h⁺ pck2::kanR pmk1-HA6H:ura4⁺ pREP3X-pck2⁺*	This work
MM846	*h⁺ pck2::kanR pmk1-HA6H:ura4⁺ pREP3X-pck2.T842A*	This work
GB35	*h⁺ pck1::ura⁺ pmk1-HA6H: ura4⁺*	Barba *et al.* (2008)
BV813	*h⁺ pck2::kanR pck2.A392E-HA:leu1⁺ pmk1-HA6H:ura4⁺*	This work
MM1746	*h⁺ pck1::ura pck1.A399E-HA:leu1⁺ pmk1-HA6H:ura4⁺*	This work
BV630	*h⁺ pck1::ura pck1.A399E-HA:leu1⁺ pmk1-HA6H:ura4⁺ pck2::natR*	This work
MM2096	*h⁺ pck1::ura pck1-HA:leu1⁺ pmk1-HA6H:ura4⁺ pck2::natR*	This work
MM1904	h⁻ *pmk1::nat ura4D-18 leu1-32*	This work
MM2119	*h? pmk1::nat pck1::ura pck1.A399E-HA:leu1⁺ pmk1-HA6H:ura4⁺*	This work
MI102	*h⁺ pmk1::kanR*	Madrid *et al.* (2006)
BV641	*h⁺ pREP3X-pck1⁺*	This work
BV643	*h⁺ pREP3X-pck1.A399E*	This work
BV645	*h⁺ pREP3X-pck1⁺ pmk1::kanR*	This work
BV647	*h⁺ pREP3X-pck1.A399E pmk1::kanR*	This work
MM2143	*h? rho1.596:natR pck1::ura pck1.A399E-HA:leu1⁺ pmk1-HA6H:ura4⁺*	This work
MM2140	*h? rho2::kanR rho1.596:natR pck1::ura pck1-HA:leu1⁺ pmk1-HA6H:ura4⁺*	This work
MM2144	*h? rho2::kanR rho1.596:natR pck1::ura pck1.A399E-HA:leu1⁺ pmk1-HA6H:ura4⁺*	This work
MM2183	*rho2::kanR pck1::ura pck1.A399E-HA:leu1⁺ pmk1-HA6H:ura4⁺*	This work
BV623	*h⁺ pck2::kanR pck2.D808N-HA:leu1⁺ pmk1-HA6H:ura4⁺*	This work
BV625	*h⁺ pck2::kanR pck2.A392ED808N-HA:leu1⁺ pmk1-HA6H:ura4⁺*	This work
BV627	*h⁺ pck1::ura pck1.D789N-HA:leu1⁺ pmk1-HA6H:ura4⁺*	This work
BV629	*h⁺ pck1::ura pck1.A399ED789N-HA:leu1⁺ pmk1-HA6H:ura4⁺*	This work
BV819	*h? rho1.596:natR pck2::kanR pck2-HA:leu1⁺ pmk1-HA6H:ura4⁺*	This work
BV822	*h? rho1.596:natR pck2::kanR pck2.A392E-HA:leu1⁺ pmk1-HA6H:ura4⁺*	This work

Table. S1 Yeast strains used in this work.
All strains are *ade- ura4D-18 leu1-32*

Oligonucleotide	Sequence 5'-3'
Pck1XbaI-F	TATAT*TCTAGA*GAGGAGATTGCATAAAGAGA
Pck1HASmaI-R	TATAT*CCCGGG*CTATGCATAGTCCGGGACGTCATAGGGATAGCCTTCAGTAGC AAAACTGGAAA
Pck1NruIX-F	TTTCGAAGT**AG**C**T**AATAAAGAAA
Pck1NruIX-R	TTTCTTTATT**A**G**CT**ACTTCGAAA
Pck1pKG-F (*Sma*I)	TATAT*CCCGGG*AATGGTGCAGTTGGATGAT
Pck1pKG-R (*Xba*I)	TATAA*TCTAGA*CTATTCAGTAGCAAAACT
Ksg1pKG-F (*Sma*I)	TATAT*CCCGGG*AATGCGAAATACGCACAAT (JCS paper Pck2)
Ksg1pKG-R (*Nco*I)	TATAT*CCATGG*TTAGACAGCACTTCTAGC
Ksg1K128R-F	AATATGCTATTA**G**GGTGTTGGATAA
KsgK128R-R	TTATCCAACACC**C**TAATAGCATATT
Ksg1K128E-F	GAATATGCTATT**G**AGGTGTTGGATA
Ksg1K128E-R	TATCCAACACCTCAATAGCATATTC
Pck1T823A-F	CAATACAACTTCC**G**CCTTTTGTGGTAC
Pck1T823A-R	GTACCACAAAAGG**C**GGAAGTTGTATTG
Pck1T827A-F	CACCTTTTGTGGT**G**CCCCCGAATTCAT
Pck1T827-R	ATGAATTCGGGGG**C**ACCACAAAAGGTG
Pck1T965A-F	TGTCCAACTTTG**G**CACCTGTCAATA
Pck1T965A-R	TATTGACAGGTG**C**CAAAGTTGGACA
Pck1S983A-F	TCAGAGGATTT**G**CCAGTTTTGCTAC
Pck1S983A-R	GTAGCAAAACTGG**C**AAATCCTCTGA
Pck1K693W-F	TTTATGCCATCTGGGTTCTGAAAAA
Pck1K693W-R	TTTTTCAGAACCCAGATGGCATAAA
Pck2A392E-F	TCGTCAAGGTG**AG**ATCCGTCAACGC
Pck2A392E-R	GCGTTGACGGAT**CT**CACCTTGACGA
Pck1A399E-F	GACGTCAAGGAG**AG**ATTCGCCAAAAG
Pck1A399E-R	CTTTTGGCGAAT**CT**CTCCTTGACGTC
Pck2D808N-F	GTATCATATACCGT**AA**TCTTAAGCTTGATAA
Pck2D808N-R	TTATCAAGCTTAAGA**TT**ACGGTATATGATAC
Pck1D789N-F	GAATTGCTTACCGT**AA**TTTGAAATTGGATAA
Pck1D789N-R	TTATCCAATTTCAAA**TT**ACGGTAAGCAATTC

Table S2. Oligonucleotides
Restriction sites are shown italicized; mutagenic sequences are marked in bold.